ST. ANTHONY FALLS LABORATORY
Engineering, Environmental and Geophysical Fluid Dynamics

Project Report No. 523

Estimation of Groundwater Inflow to the Vermillion River from Observations of Stream Flow and Stream Temperature

by

Ben Janke, William R. Herb, Omid Mohseni, and Heinz G. Stefan

Prepared for
Vermillion River Watershed Joint Powers Organization,
Dakota County, Minnesota
and
Minnesota Pollution Control Agency
St. Paul, Minnesota

November 2009
Updated: May 2010
Minneapolis, Minnesota

Abstract

A model has been developed for estimation of groundwater inflow to a stream reach from observations of stream temperature, groundwater temperature, stream flow rate, and standard weather parameters. The purpose of this model is to provide an estimate of groundwater inflow rate for stream reaches where groundwater inflow is significant. This information is useful for management of fisheries and urban development in watersheds where stream temperature is a concern. In particular, the model was developed for use in the Vermillion River, which has designated trout stream reaches that may be impacted by development in the watershed.

The model estimates groundwater inflow rate from a stream reach heat budget, which takes into account atmospheric heat flux, sediment-water heat exchange, and groundwater inflow. The model requires the following data as input: stream temperature at the upstream and downstream ends of the stream reach, stream flow at either end of the reach, standard weather data, and no significant tributaries or inflows between the ends of the reach. The model was applied to six reaches in the Vermillion River watershed.

Estimated groundwater inflow rates showed considerable spatial and temporal variability, both seasonally and between the two years simulated (2006 and 2007). In North Creek, groundwater inflow rate was 0.45 to 1.30 cfs/mile in 2007; in the upper Vermillion River main stem for the same period estimated inflow rates ranged from 0.15 to 3.87 cfs/mile. In the middle Vermillion River main stem, estimated inflow rates were unnaturally large and more variable (0.39 to 11.1 cfs/mile); these estimates include significant tributary inflow, which is lumped with groundwater inflow in the model. This, along with the failure of the model for reaches or periods involving high stream flows, is the likely source of the over-predicted groundwater inflow values. Simulations for lower South Creek showed negligible groundwater inflow for 2006; results for lower South Branch were very typical of a groundwater-fed stream, with relatively constant groundwater inflow (around 1.0 cfs/mile) that fluctuated only slightly during periods of heavy rainfall. A comparison of predicted groundwater inflow rates throughout the watershed for both dry (baseflow) and high-flow conditions suggest the presence of shallow groundwater, particularly in the lower reaches of the watershed.

The significant variability in groundwater inflow rate predicted by the model can be traced to a number of factors, including data quality and sensitivity of the model to groundwater temperatures, stream shading/sheltering, and especially to stream flow. An extensive sensitivity analysis of the model is presented in this report, as well as an analysis of available data, in particular, groundwater temperature. Limitations of the heat budget approach to modeling groundwater inflow rate are also discussed and criteria for application of the model are developed from the results of sensitivity analysis.

Table of Contents

Notation and Symbols

α_s:	reflectivity of a surface with respect to solar radiation [dimensionless]
Δx:	width of stream cell [m]
Δt:	time step [s]
ε_a:	emissivity of the atmosphere [dimensionless]
ε_s:	emissivity of stream surface [dimensionless]
ρ_a:	density of air [kg/m^3]
ρ_w:	density of water [kg/m^3]
σ:	Stefan-Boltzmann constant [kJ K^{-4} m^{-2} day^{-1}]
A:	cross-sectional area of the stream [m^2]
A_s:	surface area of the stream [m^2]
B:	mean surface width of stream, or wetted perimeter [m]
C_{fc}:	forced convection bulk transfer coefficient [dimensionless]
C_{nc}:	free (natural) convection bulk transfer coefficient [ºC$^{-1/3}$·m/s]
$C_{p,a}$:	specific heat of air [J/kg*K]
$C_{p,w}$:	specific heat of water [J/kg*K]
d:	mean or characteristic stream depth [m]
e_a:	actual vapor pressure of air [mbar]
e_s:	saturation vapor pressure of air, evaluated at stream temperature [kPa]
e_{sat}:	saturation vapor pressure of air, evaluated at air temperature [mbar]
F_c :	cloudiness factor [dimensionless]
h_{atm}:	net atmospheric heat flux [W/m^2]
h_{evap}:	heat transfer by evaporation [W/m^2]
$h_{lw,in}$:	net incoming longwave radiation [W/m^2]
$h_{lw,net}$:	net longwave radiation [W/m^2]
$h_{lw,out}$:	net outgoing longwave radiation [W/m^2]
h_s:	total incoming solar radiation [W/m^2]
h_{sed}:	heat transfer between stream and sediments [W/m^2]
$h_{s,net}$:	net incoming solar radiation [W/m^2]
K_{sed}:	sediment-water heat exchange coefficient [W/m^{2}K]
L:	stream reach length [m]
L_v:	latent heat of vaporization of water [J/kg]
q_g:	groundwater inflow rate [m^2 per mile of stream length]
Q:	volumetric stream flow rate [m^3/s]
Q_{ds}:	volumetric stream flow rate at downstream end of reach [m^3/s]
Q_g:	volumetric groundwater inflow rate [m^3/s]
Q_{ups}:	volumetric stream flow rate at upstream end of reach [m^3/s]
S:	source term in heat budget [˚C*m^2/s]
SH:	shading/sheltering coefficient [dimensionless]
t:	time [h]
$\underline{t}$:	time in moving coordinate system (Model 2) [h]
T_a:	air temperature [°C]
T_g:	groundwater temperature [°C]
T_{ref}:	reference temperature for stream-sediment heat flux formulation [°C]

T_s:	stream temperature [°C]
$T_{s,ds}$:	observed stream temperature at downstream end of reach [°C]
$T_{s,ups}$:	observed stream temperature at upstream end of reach [°C]
T_v:	virtual temperature [°C]
u:	stream velocity [m/s]
u_2:	wind speed evaluated at a height of 2m [m/s]
x:	stream-wise spatial coordinate [m]
$\underline{x}$:	stream-wise spatial coordinate in moving coordinate system (Model 2) [m]

1. Introduction

A stream temperature model has been developed to assess the impact of urban development on stream temperatures in the Vermillion River watershed (Herb, 2008; Herb and Stefan, 2008a,b). Increased surface water runoff volume and temperature, reduced groundwater recharge, and heating of shallow aquifers from paved surfaces are of particular concern (Klein, 1979; Galli, 1990; Paul and Meyer, 2001, Taylor and Stefan, 2009). The modeling tool will be useful to assess the potential impact of current and future urban development in the watershed.

The main goal of the study described in this report is to determine groundwater input (flow rate and temperature) for various reaches of the Vermillion River and its tributaries. Groundwater input is a crucial component of the stream temperature model, and information on reaches where groundwater input is significant is needed. These areas are often located in designated trout stream reaches, and need to receive particular attention when future urban development in the watershed is in the planning stage.

While groundwater temperature can be measured with relative ease using wells, estimating groundwater flow rate into a stream can be complicated. Existing methods rely on direct measurement with seepage meters, measurement of water levels in piezometers located within and adjacent to the stream, or measurements of streamflow rates at consecutive stream gaging stations. However, the distance between stream gaging stations is often so large (e.g. many kilometers) that the resolution in stream flow data is insufficient to determine groundwater input, which can be concentrated in stream reaches as short as 10 to 100 meters. The spatial variability of groundwater input can be difficult to quantify with seepage meters, which can be challenging to install in moving water, or with piezometric head data, which requires knowledge of the hydraulic conductivity of the streambed, a parameter that can vary by orders of magnitude.

In light of these difficulties, the use of temperature as a tracer for groundwater movement has become common in recent decades (Stonestrom and Constantz, 2003; Anderson, 2005; Constantz, 2008). Water temperature has been employed to identify stream reaches as “gaining” or “losing” based on comparisons of streambed temperature and stream water temperature (e.g. Silliman and Booth, 1993; Dumouchelle, 2001). Temperature differentials have also been used in conjunction with head data to estimate hydraulic conductivity and direction of movement of groundwater (e.g. Conant, 2004; Su et al., 2004), and streambed temperature profiles have been used to determine flow rates from 1-D or 2-D solutions of the heat transport equation (e.g. Bartolino et al, 1999; Essaid et al., 2008; Duque et al., 2010).

A related approach involves estimating groundwater input from the heat budget of a stream. This heat budget approach and its potential model formulations will be described in this report, as well as the application and results of the chosen formulation. This method, as all methods, has advantages and disadvantages, which will become apparent as the work is described. The biggest advantage is that the necessary resolution of water

temperature data can be supplied inexpensively using water temperature recorders commercially available from several manufacturers (HOBO, VEMCO, OMEGA and others). These self-contained units can be purchased for $10 to 200 per unit. They can operate for weeks to months and record water temperatures with time resolution from seconds to hours. The biggest disadvantage is that the groundwater input is only one of several heat flux components in the heat budget of a stream. In addition, when the water temperature difference between the stream and the groundwater approaches zero the method becomes useless. The success of any model formulation will therefore depend on the type and quality of available data. The accuracy desired and the ease of model implementation will be additional factors. Inverse modeling will be used to determine "groundwater inflow," which is the primary unknown parameter in the heat budget equation. At a minimum, the data necessary to determine "groundwater input" will include stream flow rate measured at one point in the stream or tributary, stream geometry, stream water temperatures at several points, and groundwater temperature, as well as weather parameters. All available data will be examined to assess the suitability of the data set for use in this approach to modeling groundwater inflow flow rate.

2. Field Study

2.1. Hydrogeologic Setting

The Vermillion River, a tributary of the Mississippi River located at the southern fringe of the Twin Cities metropolitan area in Minnesota, was used for a case study. The Vermillion River stream system has a number of designated trout stream reaches. Roughly 80% of the flow in the upper Vermillion River is base flow from groundwater sources (Erickson and Stefan 2008). The low stream temperatures required to maintain a viable brown trout population are generally provided by localized groundwater inputs; riparian shading is lacking in many reaches of the Vermillion River and its major tributaries.

The principal groundwater source in the Vermillion River basin is a surficial aquifer of high hydraulic conductivity. Its thickness varies generally from 25 to 100 feet, with a maximum depth of 200 feet. Some bedrock outcroppings are also present (Erickson and Stefan, 2009). Transmissivity is highest near the stream, where the surface aquifer consists primarily of coarse glacial outwash; areas of finer-textured glacial till further from the river lead to lower transmissivity values with distance from the stream (Palen, 1990a,b; EOR, 2007). The water table is just a few feet below the ground surface and the surface aquifer responds quickly to rainfall and groundwater recharge.

Below the surficial aquifer are several bedrock aquifers that can potentially leak water to the stream, including the St. Peter and Prairie du Chien aquifers. The St. Peter formation is present in the northwest part of the watershed, and consists primarily of coarse sandstone. The Prairie du Chien group consists mostly of dolomite, and underlies the rest of the watershed (Dakota County, 2006). This aquifer is largely confined except where cut by buried valleys, the deepest of which is located in the far eastern part of the watershed.

Due to the large variations in hydrogeology in the watershed, groundwater inflows to the Vermillion River are expected to be spatially variable. In addition, climatological differences between years, and errors or inconsistencies in the input data will cause temporal variability in groundwater inflows. This situation will potentially complicate the interpretation of the results.

2.2. Data Collection

Hydrologic data collection in the Vermillion River watershed, which historically has been fairly irregular, has intensified since 2000. Numerous individuals, government entities and consultants to agencies (Department of Natural Resources, Minnesota Pollution Control Agency, Metropolitan Council, Dakota County SWCD, Scott County SWCD, Vermillion River WS Joint Powers Organization, Applied Ecological Services, Emmons and Olivier Resources) have contributed to the database, which unfortunately is not assembled in one single place. Mean daily stream flow has been recorded at one USGS gaging station near Empire for nearly 30 years, and at 7 locations since 2000; stream temperature has been measured at roughly three-dozen sites since 2005. In fall of 2006, probes were installed at approximately 30 stations in the watershed to record water temperatures in the flowing stream water and in the streambed. Weather data, including air temperature, dew point, wind speed, solar radiation, and precipitation, have been collected at a number of sites, including the Rosemount Agricultural Research Station at the northern end of the watershed, at Air-Lake Airport in Lakeville, at a weather station near the Empire wastewater treatment plant, and at the St. Anthony Falls Laboratory in Minneapolis. A more complete summary of available data can be found in Appendix A.

A map of the watershed showing the locations of stream gaging stations and stations where stream and streambed (groundwater) temperature were measured at one time or another is shown in Appendix A (Figures A-1 and A-2, respectively). Stream flow gaging stations are located along the main stem of the Vermillion River and in three of the major tributaries (South Branch, North Creek, and Middle Creek). Stream and groundwater temperature loggers were placed at these locations, as well as at additional locations along the main stem and in many of the lesser tributaries. The major tributaries have multiple stations along their lengths.

The locations of the monitoring stations allow the selection of stream reaches based on the following data availability:

1) stream temperature at two locations, one at the upstream end and the other at the downstream end of the stream reach;
2) groundwater temperature at one or more locations within the stream reach;
3) stream flow or water level data at either end of the stream reach.

A one-week sample record from a 2-mile reach in the upper main stem of the Vermillion River is shown in Figure 2.1. The smaller diurnal amplitude and slight lag of the downstream water temperature relative to the upstream water temperature record indicates the presence of groundwater inflow and shading in this reach. After a small rainfall event on 8/3, the downstream temperature is elevated because of storm water

inflows near this point. Groundwater temperature remains unaffected by the rainfall event, indicating that this is a groundwater gaining reach.

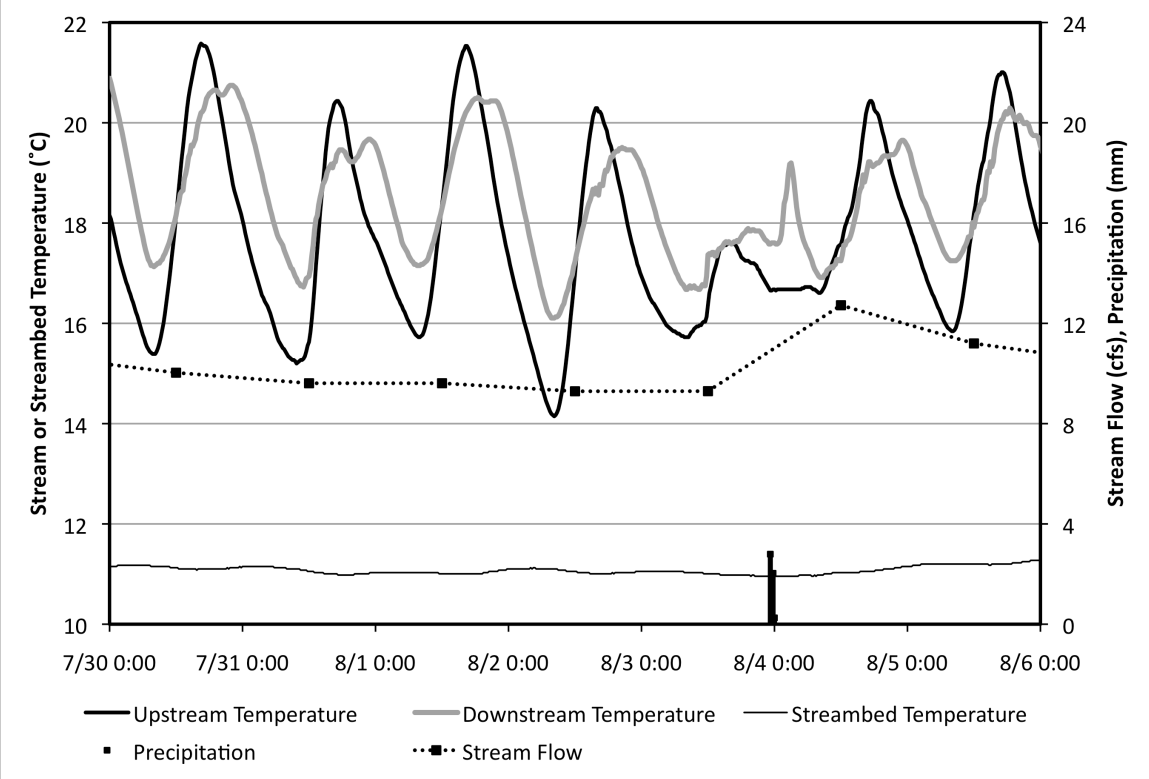

Figure 2.1. Sample of weekly data record for a 2.0 mile-long modeled reach in the upper Vermillion River, July 30 – August 6, 2008. 6.35 mm of precipitation fell just before midnight of August 4.

In addition, stream geometry data are required for each stream reach, including stream surface width, cross-sectional area (or mean depth), and bed slope. This information can be obtained from stream surveys, detailed flow measurements, and contour maps. Weather data from Rosemount or Lakeville are assumed to be representative for any stream reach within the watershed. Available data and sites for application of the groundwater model will be described later.

3. Heat and Mass (Water) Transfer Processes in a Stream

Water temperatures in a stream respond to heat transfer processes that include atmospheric heat exchange (solar/short wave radiation, long wave/atmospheric radiation, evaporation, and sensible/convective heat transfer), heat conduction between the water and the streambed/sediment, heat contained in groundwater inflow to the stream, and net heat advected by the flow in the stream. Heat stored in a stream's water (and hence stream water temperature) changes in response to the above heat fluxes. An unsteady (time-variable) heat balance for a stream reach can be written in 1-D form as:

$$\frac{\partial}{\partial t}(AT_s)+\frac{\partial}{\partial x}(QT_s)=S \qquad (1)$$

where A is the cross-sectional area of the stream [m^2], T_s is stream temperature [˚C], Q is the volumetric flow rate [m^3/s], and S is the heat source term [˚C*m^2/s]; t is time and x is distance along the stream. The source term incorporates the contributions of atmospheric heat exchange, sediment heat transfer, and groundwater inflow, and is given as:

$$S = B\frac{(h_{atm}+h_{sed})}{\rho_w C_{p,w}}+q_g T_g \qquad (2)$$

where B is the mean or characteristic stream width [m], h_{atm} is the total (net) atmospheric heat exchange [W/m^2], h_{sed} is the conductive/convective heat transfer to or from the stream sediments, q_g is the groundwater inflow rate (per length of stream reach) [m^2/s], and T_g is the groundwater temperature [˚C]. Both the groundwater inflow rate and temperature are constant (average values) along the stream reach. Although only one characteristic stream width B is shown in Eq. 2, it should be noted that B is different for the atmospheric and sediment heat transfer terms; for atmospheric heat transfer B is the stream surface width, and for sediment heat flux B is the wetted perimeter. In shallow and wide streams, the two B values are almost the same.

The mass (water) balance for a stream reach is relatively simple. The main water fluxes are stream flow Q and groundwater inflow q_g. These two water flow rates are related by the mass balance (continuity equation) for the stream reach:

$$Q_{ups}+q_g L = Q_{ds} \qquad (3)$$

where Q_{ups} is the upstream (inlet) flow rate [m^3/s], L is the total length of the stream reach [m], and Q_{ds} is the observed downstream (outlet) flow rate [m^3/s]. It assumed in this case that groundwater inflow is constant along the reach and that there are no significant tributaries in the reach to contribute flow to the mass budget. Water losses by evapotranspiration (uptake of water by plant roots) are assumed negligible.

The total (net) atmospheric heat exchange h_{atm} [W/m^2] and the conductive/convective heat transfer to or from the stream sediments h_{sed} need to be determined by separate relationships.

3.1. Atmospheric heat transfer

Two major approaches exist for characterization of the net atmospheric heat exchange at a water surface: (1) using a bulk surface heat exchange formulation with a dependence on an equilibrium temperature (Edinger 1968, 1974), or (2) using a set of equations that describe each heat flux component separately. The latter method is utilized in this model due to its generally greater accuracy, availability of necessary weather data, and the fact that additional computational requirements for this method are negligible.

A complete estimation of atmospheric heat exchange involves developing separate formulations for each heat flux component: solar (mostly short wave) radiation, atmospheric (long wave) radiation, evaporative (latent) heat flux, and convective (sensible) heat flux. The equations used for these individual heat flux components are described below.

3.1.1. Radiation

The net radiation heat flux consists of the net solar radiation $h_{s,net}$ and the net atmospheric radiation $h_{lw,net}$. The net solar radiation retained on the surface is $h_{s,net} = h_s(1-\alpha_s)$, where h_s is the total measured incoming solar radiation at the surface (W/m^2) and α_s is the surface reflectivity (Duffie and Beckman, 1991). Net long wave radiation is a measure of the heat radiated downwards by the atmosphere minus the heat radiated upwards by the ground or water surface. Incoming long wave radiation is modeled as a function of the absolute air temperature T_a (K), vapor pressure of air near the surface e_s (kPa), cloud-cover fraction F_c, and atmospheric emissivity ε_a. The Idso (1981) equation is often used to define atmospheric emissivity: $\varepsilon_a = 0.7 + 5.95 \cdot 10^{-5} e_s \cdot \exp(1500/T_a)$. We shall use a formulation proposed by Pirazzini et al. (2000) for total incoming long wave radiation, which modifies the Idso (1981) equation. Out-going long wave radiation emitted by the ground or water layer on the ground is determined by the surface (stream) temperature T_s (K) and surface emissivity ε_s. The formula for net long wave radiation becomes

$$h_{lw,net} = h_{lw,in} - h_{lw,out} = \varepsilon_a \sigma T_a^4 \left(1 + 0.4 F_c^2\right) - \varepsilon_s \sigma T_s^4 \qquad (4)$$

where σ is the Stefan-Boltzmann constant. The sign convention is such that a positive value indicates a net flux from the atmosphere into the water surface.

3.1.2. Latent (Evaporative) Heat Flux

Latent (evaporative) heat flux h_{evap} is the heat transfer with the vaporization of water, and transfer into the atmosphere. This heat flux is controlled by wind, near-surface buoyancy of the atmosphere, and atmospheric moisture both at the surface and aloft. The formulation for evaporative heat flux, taken from Stefan et al. (1980), accounts for moisture movement via both natural (buoyancy-driven) and forced (wind-driven) convection:

$$h_{evap} = \rho_w L_v (C_{fc} u_2 + C_{nc} \Delta T_v^{1/3})(e_{sat} - e_a) \qquad (5)$$

In this equation, ρ_w is the density of water (kg/m^3), L_v is the latent heat of vaporization of water (J/kg), C_{fc} is a forced convection transfer coefficient, C_{nc} is a free (natural) convection transfer coefficient (ºC$^{-1/3}$·m/s), u_2 is the wind speed measured at a height of roughly 2 m (m/s), ΔT_v is the difference in virtual temperature between the water surface and the air (°C), e_{sat} is the saturated vapor pressure of the air (mbar), and e_a is the actual vapor pressure of the air (mbar).

3.1.3. Sensible (Convective) Heat Flux

Sensible heat flux $h_{conv,atm}$ is a measure of the heat transferred with the bulk movement of any fluid; in this case the fluid is air in the atmosphere, and it is moved by both mean wind and buoyancy effects. This heat flux is characterized by use of the Bowen ratio (Bowen, 1926; Rasmussen et al., 1995), which relates convective heat flux to evaporative heat flux. Applying the Bowen ratio to the evaporation equation (Equation 5) results in the following formulation:

$$h_{conv,atm} = \rho_a C_{p,a}(C_{fc}u_2 + C_{nc}\Delta T_v^{1/3})(T_s - T_a) \quad (6)$$

where ρ_a is the density of air (kg/m^3), $C_{p,a}$ is the specific heat of air (J/kg·K), T_s is the water surface temperature (˚C), T_a is air temperature (˚C), and the other parameters are as defined previously. The transfer coefficients are the same as in the evaporation equation (Equation 5).

3.2. Sediment heat transfer

The heat flux across the sediment surface at the bottom of a stream can be estimated by relationships ranging from simple bulk-transfer equations to models that utilize temperature gradients in the streambed. Given that heat transfer into and out of the streambed is not usually a large component of the heat budget of a stream reach, a heat conduction equation similar to that employed in the SNTEMP stream temperature model is used (Theurer et al., 1984). Heat exchange between the sediment and stream water is assumed to be linearly proportional to the difference between stream temperature T_s and the source temperature T_{ref} representative of the streambed temperature:

$$h_{sed} = \frac{K_{sed}}{\Delta z}\left(T_{ref} - T_s\right) \quad (7)$$

where K_{sed} is the sediment-water heat exchange coefficient [W/m/K] and Δz is the distance between the stream-sediment interface and the location of the source temperature. K_{sed} has a value of about 1.65 W/m/K (Theurer et al., 1984). In our study the source temperature is a streambed temperature when possible, measured at a depth (Δz) of roughly 0.5 m. Otherwise the mean stream temperature for the period of interest is used, lagged by 36 hours (the approximate time required for a temperature pulse to conduct 0.5 m into the streambed).

4. Model Development

The main modeling objective is the prediction of groundwater flow rate into or out of a stream reach. This will be the primary unknown in the heat and mass budget equations for the stream reach, regardless of the complexity of the model formulation. Secondary

parameters to be estimated will include groundwater temperature and canopy shading, and to a lesser extent, wind sheltering.

Groundwater temperature is considered an unknown although it has been measured directly at several locations in the watershed, due to a number of issues that have cast doubt on the representativeness, and sometimes accuracy of these measurements (see Appendix B). The measurements are point measurements and provide a likely range of groundwater temperatures for a stream reach.

Canopy shading by trees and other tall plants is an important parameter because it attenuates solar radiation, the most significant source of heat to a stream. Wind sheltering, which represents the degree to which wind speed is reduced by flow through a canopy, can be crucial in the absence of solar radiation (i.e. at night) due to its influence on sensible and latent heat transfer. It is not uncommon to assume that sheltering and shading are equal, and such an assumption might be appropriate in this model.

The modeling formulations proposed and used in this study will include three unknowns: (1) groundwater flow rate, (2) groundwater temperature, and (3) stream shading/sheltering, which will be determined by model fitting to data. Any stream reach modeled will be assumed short enough such that all three parameters will be constant along the reach. The following modeling approaches are considered, in order of increasing complexity.

4.1. Model 1: Simple 'bathtub' model

A simple approach to estimating groundwater inflow to a stream reach is to assume that the entire reach behaves as a single well-mixed cell ('bathtub') in which all thermal and hydrologic inputs are well-mixed before reaching the outlet. Stream geometry is assumed constant along the entire reach, and physical dimensions are represented by average or representative values. Steady-state is also assumed. The assumptions of constant geometry and steady-state reduce the general heat transport equation (Eq. 1) to the form:

$$Q_{ups}T_{s,ups} + Q_g T_g + \frac{S \cdot A_s}{\rho_w C_{p,w}} = Q_{ds}T_{s,ds} \qquad (8)$$

where $T_{s,ups}$ is the observed stream temperature at the upstream end of the reach [˚C], $T_{s,ds}$ is the observed stream temperature at the downstream end of the reach [˚C], A_s is the surface area of the stream reach [m^2], Q_g is the groundwater inflow rate in m^3/s (the product of the per-length groundwater flow rate, q_g, and the reach length, L), and the other terms are as defined previously. The source term in this case consists of the atmospheric heat exchange and sediment-water heat transfer. The atmospheric heat flux can be determined using the full set of equations with hourly weather parameters and stream temperature, and averaging the heat flux over the entire interval of analysis.

Due to this formulation's relatively crude treatment of heat transport along a stream reach, it is perhaps most useful for determining a magnitude or likely range of values for

the groundwater inflow rate and temperature. It has the advantage of being easily applied using mean stream flow and hourly weather and stream temperature data; however, it cannot be applied at any time scale less than the travel time due to the fact that complete mixing is assumed.

4.2. Model 2: Model with moving reference frame

A second modeling approach involves ignoring dispersion effects and assuming the frame of reference moves at the mean velocity of the flow, essentially eliminating the advection term from the heat budget (Eq. 1). This assumption is analogous to considering a single parcel of water and tracking the heat fluxes into or out of the parcel as it travels from the upstream end to the downstream end of the reach. The model is essentially an advective model, and the method is similar to a method of characteristics.

Assuming constant geometry and applying the chain rule to the advection term, the heat transport equation becomes:

$$A\frac{\partial T_s}{\partial t} + T_s\frac{\partial Q}{\partial x} + Q\frac{\partial T_s}{\partial x} = \frac{B\cdot S}{\rho C_p} + q_g T_g \qquad (9)$$

From the mass balance it is known that the change in flow along the stream reach, $\delta Q/\delta x$, is equal to the per-length groundwater inflow rate, q_g. Applying this relation and dividing through by the cross-sectional area, A, results in the advective heat transport equation:

$$\frac{\partial T_s}{\partial t} + u\frac{\partial T_s}{\partial x} = \frac{S}{d\cdot \rho C_p} + \frac{q_g}{A}\left(T_g - T_s\right) \qquad (10)$$

where u is the stream velocity [m/s] and d is the mean or characteristic stream depth [m]. If the frame of reference is assumed to move with stream velocity u, the equation must be transformed to reflect this change in position with time. The new x coordinate becomes $\underline{x} = x - u\underline{t}$, with $u\underline{t}$ representing the distance traveled by the moving origin in time, $\underline{t}$. Time remains unchanged ($\underline{t} = t$), as a moving reference frame has no effect on time. The spatial derivative remains unchanged (i.e., $d/dx = d/d\underline{x}$), but the temporal derivative, d/dt, becomes $-ud/d\underline{x} + d/d\underline{t}$. Substituting these derivatives of the transformed coordinate system into the heat budget equation above eliminates the advection term, leaving a simplified equation of the form:

$$\frac{\partial T_s}{\partial t} = \frac{S}{d\cdot \rho C_p} + \frac{q_g}{A}\left(T_g - T_s\right) \qquad (11)$$

This equation can then be discretized with a simple forward-difference approximation of the time derivative:

$$\frac{T_s^{n+1} - T_s^n}{\Delta t} = \frac{S(\overline{T}_s)}{d \cdot \rho C_p} + \frac{q_g}{A}\left(T_g - \overline{T}_s\right) \qquad (12)$$

where n represents the time level, Δt is the travel time for the reach of interest, and $S(T_s)$ is used to show that the other heat fluxes are calculated using observed stream temperature, T_s, which has been averaged over time levels n and $n+1$. The depth and cross-sectional area are computed from the mean flow in the reach, which is dependent on the chosen groundwater inflow rate, q_g. Because of the moving origin, the change in stream temperature experienced by the parcel of water over the travel time (left-hand side of Equation 12) is equivalent to the difference in stream temperature between the downstream end of the reach, and the upstream end lagged by the travel time.

An iterative procedure is required to solve the equation due to the fact that stream geometry and travel time are a function of groundwater flow rate, which is the only unknown. If a guess is made for groundwater flow rate, Equation 12 can be easily solved for the final stream temperature, T_s^{n+1}. This computed temperature should be the same as the downstream temperature observed at a time Δt after the upstream temperature. If the predicted downstream (final) temperature does not match the observed temperature, the groundwater flow rate is adjusted until the computed and observed downstream temperatures match.

This model has the advantage of allowing a finer time scale to be used for analysis relative to Model 1, although it can still be run using mean daily values of input parameters (i.e. mean lagged upstream temperature, mean downstream temperature, etc.)

4.3. Model 3: Cells-in-series model

A third approach to modeling groundwater input is to visualize the stream reach as a series of adjacent cells of length Δx (Figure 4.1). Within each cell, geometry and flow (both stream flow and groundwater flow) are assumed constant. Travel time within a cell is assumed short enough that weather parameters will be roughly constant over the time steps used (quasi-steady state). Each cell is assumed to be well-mixed, such that stream temperature is constant within each cell; it varies only from cell-to-cell, i.e. stepwise with distance x along the stream. Inflow from any tributaries is neglected as in the previous formulations. The heat and mass balances for a single cell are shown in Figure 4.1.

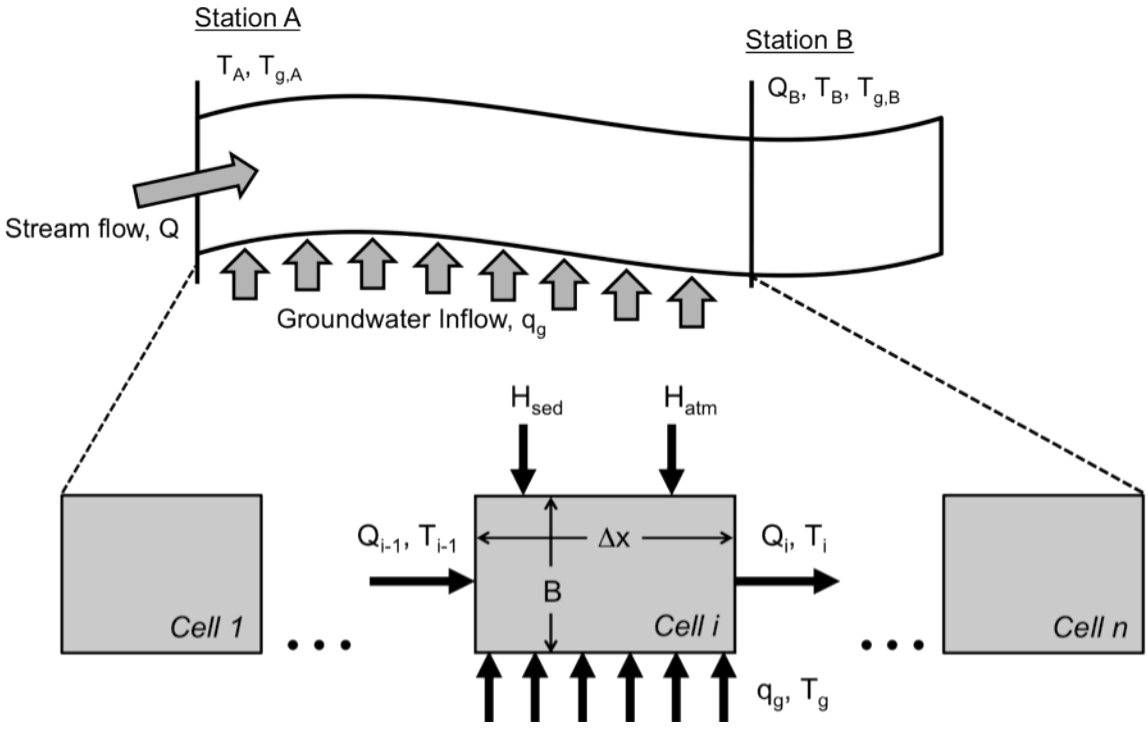

Figure 4.1. Schematic of the cells-in-series model as applied to a stream reach. The stream reach is divided into *n* cells of length Δx and width *B*. Stream temperature (*T*), streambed temperature (T_g), and stream flow (*Q*) data are collected at selected stations. H_{atm} = net heat flux across the water surface, H_{sed} = diffusive heat flux across the sediment surface, and q_g = groundwater inflow rate per unit length.

The heat budget equation (Eq. 1) is discretized using a forward-difference approximation for the time derivative (storage term) and a forward-difference Crank-Nicholson scheme for the spatial derivative (advection term). Application of these schemes results in the following form of the governing equation for some cell, *i*, within the stream reach at some time level, *k*:

$$\left(\frac{(Q_i^k T_{s,i}^k - Q_{i-1}^k T_{s,i-1}^k) + (Q_i^{k+1} T_{s,i}^{k+1} - Q_{i-1}^{k+1} T_{s,i-1}^{k+1})}{2\Delta x}\right) + S = A\left(\frac{T_{s,i}^{k+1} - T_{s,i}^k}{\Delta t}\right) \qquad (13)$$

where *k* is the time level and *S* is the heat source term, which is defined by Eq. 2 and evaluated using a cell temperature ($T_{s,i}^k$). If a steady-state version of the model is used, the right-hand side of Eq. 13 would be neglected.

Eq. 13 can be used to solve explicitly for the stream temperature T_s in cell *i*, provided that a guess is made for the groundwater flow rate q_g. In this way the equation can be applied in sequence to each cell within a reach, beginning at the upstream end and ultimately producing a temperature at the outlet of the reach. This predicted outlet temperature is then compared to the observed temperature at the outlet; if the temperature difference is within some specified tolerance, the model proceeds to the next time step. If the temperature difference is unacceptable, a new guess is made at the groundwater flow rate

and the calculation sequence is repeated to produce a new outlet temperature. This process is repeated until acceptable agreement exists between the simulated and observed stream reach outlet temperatures. Generally after the first few time steps this iteration procedure does not have to be repeated.

This model formulation is considerably more detailed than the previous models, allowing for spatial (stream-wise) variation in sediment and atmospheric heat flux, as well as in stream geometry, which would be expected to vary along a stream reach of any length. The model can be operated for either unsteady or steady-state conditions, allowing it to potentially capture temporal variability in heat inputs to a stream.

4.4 Modeling Constraints

Additional factors must be taken into consideration before the models are applied. First, since the groundwater flow is effectively being calculated as a residual of the heat budget, the model should be applied to a reach where groundwater input is expected to be significant relative to the stream flow. This is necessary to ensure that the computed flow rates are greater than the error inherent in the input data, i.e. for a small groundwater flow, it would not be known whether this flow actually exists or if it is a byproduct of some error in the input data that has been amplified through the model calculations. This implies that the model is likely to perform poorly for reaches or periods with large stream flows.

Similarly, the model should be applied during time periods when a significant difference exists between stream temperature and groundwater temperature, such as during late summer. This is also to ensure that the groundwater contribution to the heat budget is unmistakable. If stream temperature and groundwater temperature are nearly identical, it will be impossible to determine how much groundwater is present since it will not appreciably change stream temperature, even for a large groundwater flow.

Another potential source of error in the simulation results is tributary and storm water inflows, which are not accounted for in the model; the residual of the stream heat budget is completely attributed to the groundwater inflow, and not to errors in the data or to the presence of surface inflows. To separate the residual into components for groundwater and surface water (small tributary) inflows, flow and water temperature measurements in the surface inflows would be required. Without this information, the model will lump these additional flows into the estimated groundwater inflow rate, therefore over-predicting its “true” value. Thus for best results, the model should be applied (1) for reaches without any large, persistent tributaries or other surface inflows, and (2) during relatively dry weather conditions, when surface inflows (e.g. from storm water outlets, drainage ditches, or overland runoff) are minimal.

4.5 Required Model Input Data

The required data input to run the model can be summarized as follows:

1) *stream temperature* at two locations, one at the upstream end of the stream reach of interest, and one at the outlet;
2) *groundwater temperature* at a minimum of one location within the stream reach of interest, though most likely it will be measured at the same locations as stream temperature;
3) *stream flow* or gage data at either end of the stream reach;
4) *weather data* (solar radiation, air temperature, dew point temperature, and wind speed), preferably measured in the immediate vicinity of the stream reach;
5) *stream geometry*, including wetted width and stream reach length, with width representing average values over the reach of interest or taken from a representative cross-section.

If these data are available, then after consideration of the aforementioned model constraints the model can be applied to estimate groundwater inflow rate to a stream reach on a continuous basis for the period during which the data were collected.

4.6 Model Selection and Numerical Solution

After preliminary application of the three potential models to a reach in North Creek (results not shown), it was decided that Model 3 was likely to provide the most accurate results, given its ability to handle unsteady conditions and allow for spatial (stream-wise) variability of stream geometry and atmospheric heat flux. These features in particular proved crucial, since the distribution of stream temperature and gaging stations in the watershed meant that modeled stream reaches would have lengths on the order of 1-3 miles. Therefore travel times would be significant, and the assumption of steady-state (required by Model 1) would fall short of reality. Furthermore, the data input requirements of Model 3 were not any more extensive than the other two formulations, and additional computation time required by the model was negligible.

An additional requirement of Model 3 was specification of cell size (Δx) and time step (Δt) for the solution. Given that the heat and water (mass) balance equations were solved using an explicit (rather than implicit) formulation for outlet stream temperature, the relationship of the flow velocity (u) in the stream, time step, and cell size had to be considered; in general for the numerical scheme used, $u^*\Delta t/\Delta x < 0.5$ for the solution to be stable. For stream flows typically observed in the Vermillion River, a cell size of 200 m and a time step of 1.5 min were suitable for most scenarios.

Weather data was available at one-hour resolution, while stream temperature was usually available at 15-minute intervals. Stream temperature was averaged over 1-hour periods to match the interval of the weather data. Mean daily stream flows were input to the model, but linear interpolation was used to provide hourly flow values so that a step-change in flow did not occur at midnight each day, which tended to create instabilities in the simulation results.

Groundwater inflow rate was held constant for each day of analysis but allowed to vary from day to day. This was done to account for the potentially rapid response of shallow

groundwater suspected to be present in some parts of the system. These daily values of groundwater inflow rate were then averaged over the periods of analysis, which in the case of this study was a half-month. This period was selected because it approximates the maximum amount of time groundwater temperature can be assumed constant (see Appendix B). The computed groundwater inflow rate could show considerable variation, even within a single period of analysis; for example, when applied to the upper Vermillion River main stem in August 2007, the mean estimated groundwater inflow rate was 0.48 cfs/mile, with a standard deviation of 0.47 cfs/mile. This much variability is likely due to sensitivity of the model to input parameters, in particular stream temperature and weather variables, and small changes in these quantities could have an impact on groundwater inflow rate. Simulation results and a sensitivity analysis of the model are presented in Section 6.

5. Selection of Stream Reaches

Stream reach selection was based largely upon location of monitoring stations and availability of suitable data, in addition to minimizing the number of tributaries along the reach of interest, as these are not included in the model formulation. Six reaches that are suitable for application of the model are described here (see Figure 6.1 for a watershed map showing locations of modeled reaches).

5.1. Reach 1: North Creek

North Creek is perhaps the most logical stream reach to which to apply the model, because it has no significant tributaries between stream/ground water temperature monitoring stations. The model was applied to a reach of North Creek between stations AES-66 and AES-65, just upstream of the Middle Creek – North Creek confluence (Figure 5.1). Stream and groundwater temperatures were measured at AES-65, and 2.4 miles upstream at AES-66. A gaging station (NC808) was located near AES-65. There appears to be significant groundwater inflow in the middle of this reach, and there are few gaps in the groundwater and stream temperature records. North Creek has a low slope, which will lead to a relatively long travel time. Stream geometry was acquired from stream flow measurements near NC808, where depth was recorded at high spatial resolution across the channel. A number of these measurements (for both low and high flows) were available to determine a characteristic cross-sectional geometry for the reach.

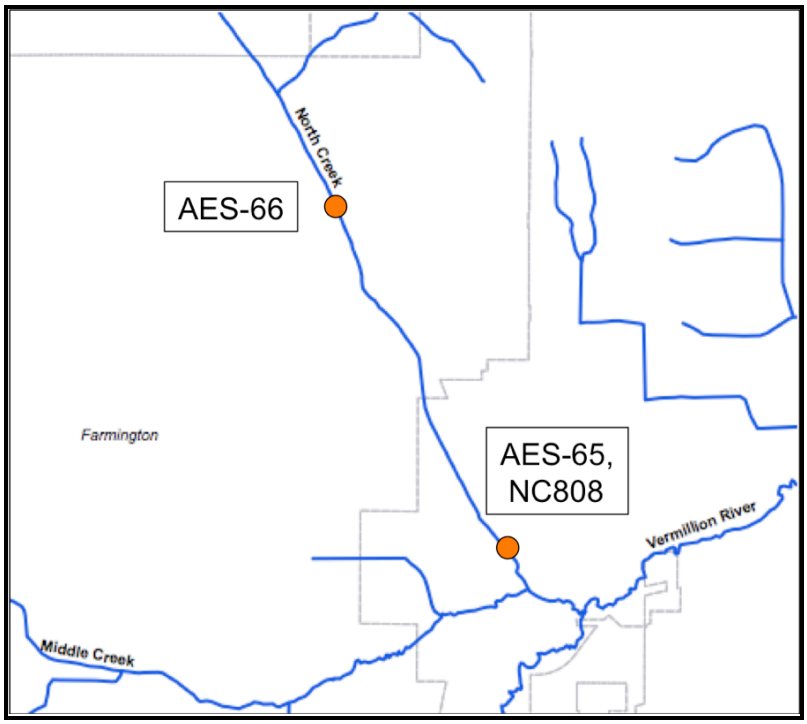

Figure 5.1. Reach 1 on North Creek; model will be applied between AES-66 and AES-65. Flow has been monitored near AES-65 (NC808).

5.2. Reach 2: Lower South Creek

Another stream reach for model application is located on the lower portion of South Creek, just upstream from the confluence with the main stem of the Vermillion River. The modeled stream reach is between temperature stations AES-84 and AES-80 (Figure 5.2), and has a length of approximately one mile. Although this reach seems ideal for model application due to the absence of major tributaries and presence of observed low stream temperature temperatures, presumably from significant inflow of groundwater or tile drainage, the lack of a flow gaging station in the reach is a big handicap. To fill in missing information, the flow rate in South Creek before its confluence with the Vermillion River was calculated as the difference between the flow measured in the Vermillion river main stem just downstream of the confluence (VR807) and that measured just upstream of the confluence (SC804). This rough estimation of flow could be a source of error. The lack of flow measurements is accompanied by a lack of geometry information, and a cross-section similar to that of North Creek was assumed.

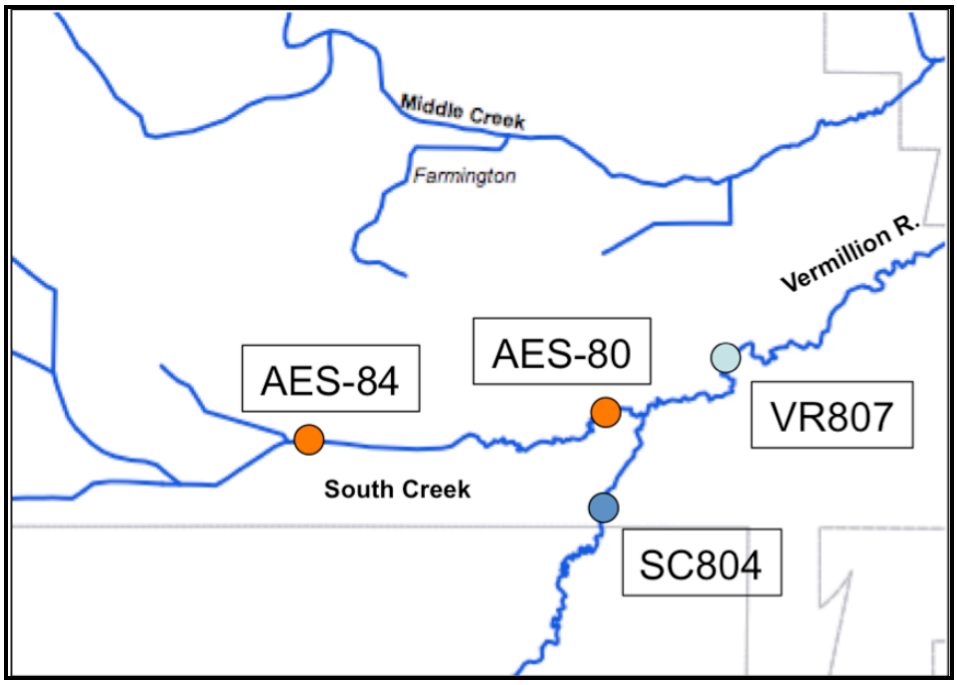

Figure 5.2. Reach 2 on lower South Creek; model will be applied between stations AES-84 and AES-80, with flow estimated as the difference between measurements at VR807 and SC804.

5.3. Reach 3: Upper Main Stem of the Vermillion River

A third stream reach suitable for analysis is located on the upper main stem of the Vermillion River, between the confluences with North Creek and South Creek. The modeled stream reach is between stations AES-79 and CHP-1, the latter of which records stream temperature only (Figure 5.3). A gaging station (VR807) is also located at AES-79. This reach, which is roughly 2 miles of designated trout stream, has no major tributaries, and was identified in a study by Emmons and Olivier Resources as a groundwater 'gaining' reach (2007). This is perhaps the only reach along the main stem of the Vermillion River where the model could be readily applied, given that other reaches of the main stem have significant tributary inflows between monitoring stations. Geometry information was taken from a number of flow measurements made at VR807.

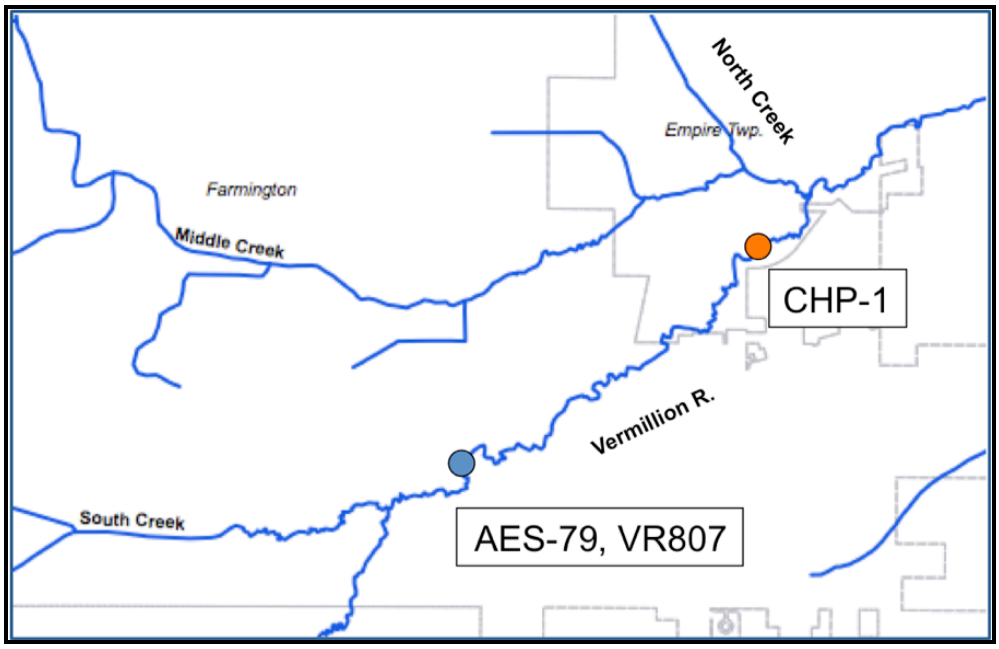

Figure 5.3. Reach 3 on the upper Vermillion River main stem; model will be applied between Stations AES-79 and CHP-1. Flow has been monitored at VR807.

5.4. Reaches 4 and 5: Middle Main Stem of the Vermillion River

The model will also be applied to sections of the middle main stem of the Vermillion River upstream and downstream of the USGS gaging station located where Blaine Avenue crosses the river. A temperature station, AES-56, has been installed at this location. The stream reach will be modeled in two sections: one section (Reach 4) from AES-58 to AES-56, and another section (Site 5) from AES-56 to AES-49, which is just upstream of the confluence of South Branch with the main stem (Figure 5.4). Reach 4 is roughly 2.3 miles long and was identified by the EOR study as a 'significant gaining reach', while Reach 5 is about 3.6 miles long and was not included in the EOR study. The entire reach includes a number of significant surface water tributaries, and this has to be considered when the results are interpreted. The stream bathymetry for this reach was slightly more difficult to obtain because the flow data come from the USGS station, and cross-sectional data are not available. Stream geometry was estimated from point flow measurements taken at VR-803, located a few miles downstream of AES-49.

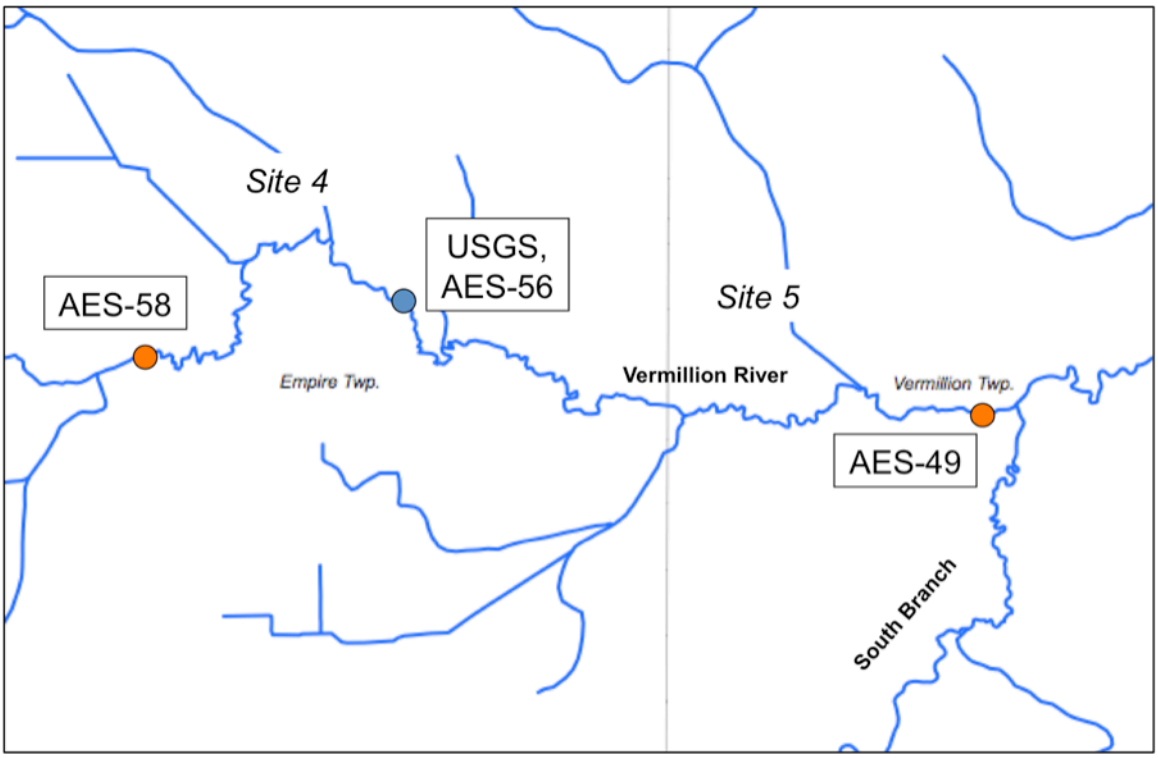

Figure 5.4. Reaches 4 and 5 on the middle Vermillion River main stem; the model will be applied between Stations AES-58 and AES-56 (Reach 4), and between AES-56 and AES-49 (Reach 5). Flow has been recorded by the USGS at a station located at AES-56.

5.5. Reach 6: Lower South Branch

A sixth reach favorable for model application is a section of South Branch just upstream of where it flows into the main stem of the Vermillion River. The model will be applied between stations AES-23 and AES-21, which is a distance of roughly 2.9 miles (Figure 5.5). A few small tributaries are present in this reach but are not expected to impact the results significantly. Flow has been measured at SB802 (located at AES-21), and stream bathymetry will come from point measurements made at this gaging station. South Branch was not included in the EOR study and therefore not designated as a gaining or losing reach, but a portion of this reach is a designated trout stream.

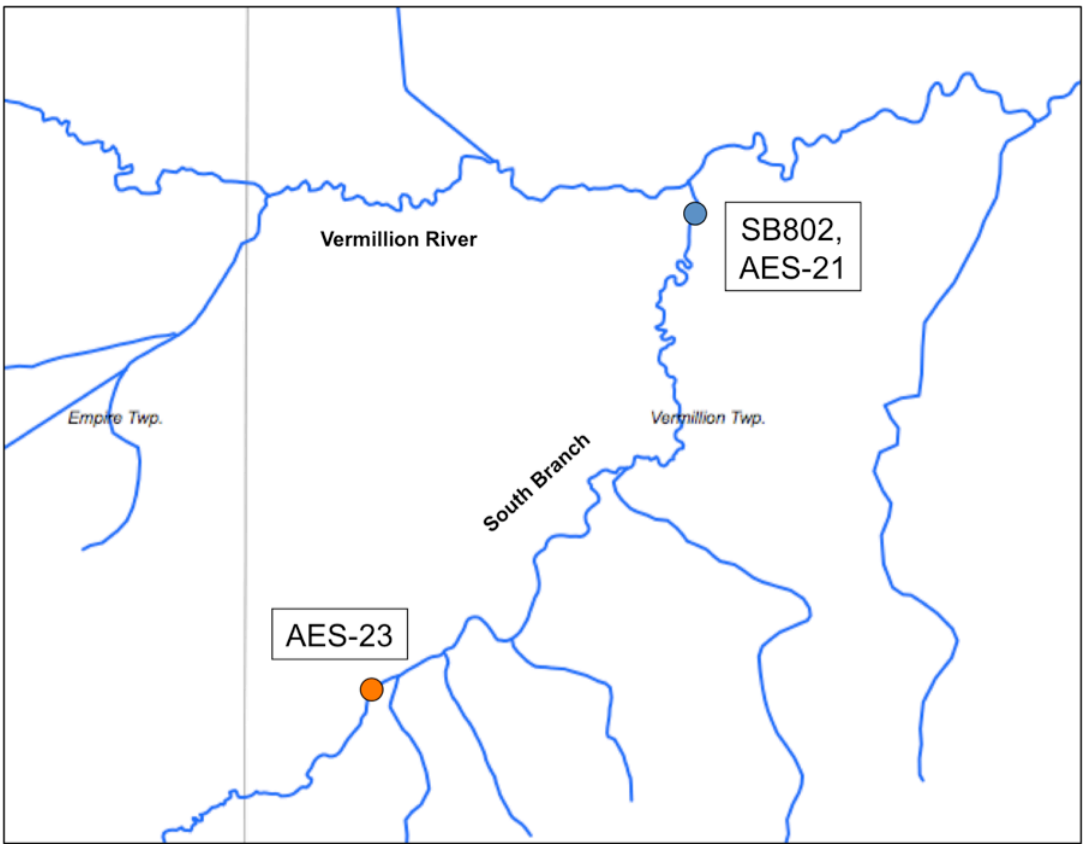

Figure 5.5. Reach 6 on the lower South Branch; model will be applied between Stations AES-23 and AES-21. Flow has been recorded at SB802.

6. Results

The main unknown to be determined from the balance equations is the groundwater inflow rate, with groundwater temperature and shading/sheltering coefficient as secondary unknown parameters.

In stream temperature modeling, shading/sheltering is typically chosen by modifying its value until the diurnal amplitude of the predicted stream temperature matches that of the observed stream temperature, without regard to mean value of temperature (which is controlled by groundwater input and/or sediment heat flux). This technique could not be used in this model since the groundwater inflow rate was not held constant. Instead shading/sheltering was estimated from aerial photography.

The groundwater temperature data collected in the Vermillion River and its tributaries had significant limitations, primarily due to installation of the temperature probes in piezometer tubes in which convective currents could take place. Therefore a mean and likely range of groundwater temperature values was computed for each modeled reach as a function of time, and simulations were run for that range of values. Appendix B

includes a more detailed analysis of the groundwater temperature data and determination of the best-guess groundwater temperatures.

Three sets of results are presented here: (1) the predicted groundwater inflow rate to the stream reach as a function of time for the simulation periods (generally September-October 2006, June-September 2007, and June-September 2008), (2) the sensitivity of predicted groundwater inflow rate to groundwater temperature and shading/sheltering for selected time periods, and (3) the relationship between estimated groundwater inflow rate and both atmospheric heat transfer and/or upstream-downstream temperature difference.

The cells-in-series version of the model was used in these simulations, due to limitations of the other two formulations. Limitations of the model in general and difficulties in application will be discussed in Section 7.

At least three extraneous events may have affected the groundwater inflow estimation, and should be acknowledged here:

(1) Dewatering flows from construction sites near the Reach 1 in North Creek likely led to an over-prediction of groundwater inflow rates in 2008.
(2) The treated effluent from the Empire wastewater treatment plant that had been discharged to the Vermillion River several miles upstream of Reach 4, the main stem reach upstream of the USGS gauging station, was permanently diverted in a pipeline to the Mississippi River in March 2008. This effluent had contributed a relatively steady 10-15 cfs to the Vermillion River main stem at an unknown temperature, and the disappearance of this flow in 2008 might explain some of the differences between the 2007 and 2008 groundwater inflow results for Reach 4.
(3) A change in the datum for the stream gauging station in the South Branch tributary between the 2007 and 2008 modeling periods led to a new flow rating curve for 2008, and the resulting discrepancy in flows likely had an effect on the estimated groundwater inflow rates for Reach 6.

6.1. Best Estimates of Groundwater Inflow Rates

6.1.1. Reach 1: North Creek

Simulations were run for North Creek using best-estimate values of groundwater temperature for 2006 and 2007 (Table B-5) and groundwater temperature observations for 2008. Shading was estimated at roughly 33%. Results are given in terms of average groundwater inflow rate (cfs per mile of stream reach) for half-month periods and as a percentage of the measured stream flow at the downstream end of the reach (Table 6.1). Also shown are measured stream flow and total precipitation per simulation period.

The simulation results in Table 6.1 suggest that North Creek receives significant groundwater inflow (0.96 cfs/mile on average), and that this inflow is highly variable with time (ranging from 0.45 cfs/mile to 1.45 cfs/mile with a standard deviation of 0.32 cfs/mile.) The results from 2006 are more consistent, but this is a consequence of a shorter data record and a very dry fall period.

Table 6.1. Estimated groundwater inflow rate (Q_g) to North Creek (Reach 1) in 2006 - 2008. Calculated from observations of stream flow, stream temperature and weather, and using prescribed groundwater temperature (2006-2007) or observed groundwater temperature (2008). Total precipitation and mean measured stream flow (Q_s) per period are also shown.

Period	Qs (cfs)	Precip (cm)	Tg (°C)	Qg (cfs/mi)	Qg (% Qs)
2006					
Sep 16-30	4.6	1.36	12	1.4	71
Oct 1-15	4.5	0.41	11	1.2	67
Oct 16-31	3.2	0.10	10	1.1	85
2007					
June 1-15	10.5	1.72	10	0.57	13
June 16-30	7.5	2.24	10	0.66	22
July 1-15	8.1	2.69	11	0.45	13
July 16-31	5.5	0.25	12	0.83	38
Aug 1-15	4.1	7.57	13	0.72	55
Aug 16-31	20.8	9.96	14	0.78	10
Sep 1-15	3.7	3.48	15	1.30	82
Sep 16-30	3.3	8.56	14	0.68	60
Oct 1-15	13.7	6.35	13	0.94	18
2008					
June 1-15	21.2	6.81	12.9	0.64	12
June 16-30	8.0	0.23	13.3	0.79	28
July 1-15	5.8	3.00	13.6	1.44	65
July 16-31	4.5	1.40	13.9	1.45	77
Aug 1-15	3.5	2.54	13.8	1.44	97
Aug 16-31	2.7	3.53	14	1.07	95
Sep 1-15	2.6	2.72	13.5	0.86	82
Sep 16-30	2.8	2.87	13.3	0.91	82

Since storm water surface runoff is not accounted for in the model, periods with a large amount of rainfall may produce more erroneous groundwater inflow results; this is likely the case for August 2007 when heavy rains occurred in Minnesota. The large groundwater inflow in early September suggests a fast coupling (short lag) between the shallow groundwater system and the stream flow in the North Creek watershed. The same response occurs again when large groundwater inflows in October lag behind rainy periods in August and September 2007. This trend does not show up in 2008, perhaps mostly due to the drought-like conditions for most of the summer and fall of that year.

As expected, groundwater inflow makes up a greater percentage (60-80%) of stream flow during low-flow periods. This result is consistent with the findings of the EOR (2007) study that identified North Creek as a significant gaining reach.

6.1.2. Reach 2: Lower South Creek

The analysis of South Creek was limited to 2006 because downstream temperature data for station AES-80 were not available for 2007 or 2008. Shading/sheltering was

estimated to be 25%, and groundwater temperature was as determined in Appendix B. Results are shown in Table 6.2.

Table 6.2. Estimated groundwater inflow rate (Q_g) to lower South Creek (Reach 2) in 2006. Calculated from observations of stream flow, stream temperature and weather, and using a prescribed groundwater temperature. Total precipitation and mean measured stream flow (Q_s) per period are also shown.

Period	Qs (cfs)	Precip (cm)	Tg (˚C)	Qg (cfs/mi)	Qg (% Qs)
2006					
June 1-15	13.0	1.79	8	0.0	0
June 16-30	14.2	2.34	9	0.0	0
July 1-15	11.0	0.94	10	0.0	0
July 16-31	10.7	1.55	11	0.00	0
Aug 1-15	17.0	5.50	12	0.00	0
Aug 16-31	10.4	2.3	13	0.04	0
Sep 1-15	9.5	1.0	13	1.70	19

With the exception of one simulation period, the model predicted no significant groundwater inflow to lower South Creek, which apart from being a questionable result, is contrary to the EOR study (2007) that identified South Creek as a 'gaining' reach. A number of factors could be contributing to this result: stream flow was not measured directly, and a cross-section similar to that of North Creek was assumed. More importantly, however, the measured stream temperatures are lower at the upstream station (AES-84) than at the downstream station (AES-80); the difference is 2.2 ˚C on average for the year and a maximum of 4.9 ˚C. Since groundwater temperature is nearly always lower than stream temperature during summer and fall (even in this relatively cold stream reach), atmospheric forcing has to account for the 2.2˚C water temperature increase from the upstream to the downstream station. Even with groundwater contribution set to zero, the modeled stream temperature at the outlet was lower than what was observed. This suggests an error in the model itself or in the input data, with the latter likely involving the observed stream temperatures. For example, the upstream station may be at a location where a spring enters the stream, or the downstream probe may have been placed too close to the surface of the stream. It should also be mentioned that a drainage tile system connects to South Creek a mile or two upstream of the analyzed stream reach; it keeps stream temperatures low relative to the rest of the entire watershed. Groundwater is also known to enter the system in the upper reaches of South Creek. Thus it is possible that the model results are accurate and that very little groundwater enters lower South Creek in the modeled reach, with low temperatures maintained instead by cold flow from upstream. This would also explain the low temperatures measured at the upstream end of the modeled reach.

6.1.3. Reach 3: Upper Main Stem of the Vermillion River

Simulations were run for a section of the upper Vermillion River main stem from station AES-79 to CHP-1 for 2006 to 2008. This is the only reach for which data existed for the

summer months (June-August) for all three years. Shading/sheltering was estimated to be 75% for this reach, which is heavily shaded. Results are shown in Table 6.3.

Table 6.3. Estimated groundwater inflow rate (Q_g) to the upper Vermillion River main stem (Reach 3), 2006 - 2008. Calculated from observations of stream flow, stream temperature and weather, and using a prescribed groundwater temperature (2006-2007) or observed groundwater temperature (2008). Total precipitation and mean measured stream flow (Q_s) per period are also shown.

Period	Qs (cfs)	Precip (cm)	Tg (°C)	Qg (cfs/mi)	Qg (% Qs)
2006					
June 1-15	15.2	1.79	8	0.16	2
June 16-30	20.8	2.34	9	0.26	2
July 1-15	13.2	0.94	10	0.14	2
July 16-31	11.5	1.55	11	0.18	3
Aug 1-15	22.8	5.50	12	0.29	3
Aug 16-31	13.6	2.3	13	0.26	4
2007					
June 1-15	11.7	1.72	10	0.15	3
June 16-30	9.3	2.24	11	1.19	19
July 1-15	5.3	2.69	12	2.12	44
July 16-31	4.1	0.25	13	1.91	49
Aug 1-15	8.7	7.57	13	1.12	29
Aug 16-31	29.9	9.96	14	0.90	6
Sep 1-15	19.9	3.48	14	2.20	17
Sep 16-30	20.0	8.56	13	2.80	19
Oct 1-15	27.3	6.35	13	3.87	20
2008					
June 1-15	55.7	6.81	10.4	1.46	5
June 16-30	25.3	0.23	10.5	0.41	3
July 1-15	17.9	3.00	10.9	0.57	6
July 16-31	12.3	1.40	11	0.33	6
Aug 1-15	9.4	2.54	11.1	0.50	10
Aug 16-31	7.3	3.53	11	0.92	21
Sep 1-15	8.3	2.72	10.7	1.15	19
Sep 16-30	8.8	2.87	10.8	1.16	19

As for the other two stream reaches, the results suggest a variable groundwater inflow to the stream; values ranged from 0.14 to 3.87 cfs/mile for the whole record and the standard deviation (0.98 cfs/mile) was nearly as large as the mean flow (1.05 cfs/mile). Also of note are consistently low values in 2006 and to an extent in 2008, with the latter likely the result of 2008 being a much drier year than 2007. The EOR study (2007) identified this section of the Vermillion River as a 'gaining' reach, which is roughly consistent with the results shown here.

The discrepancy between years suggests some error in the input data, perhaps in the observed stream temperatures. Estimated groundwater inflow rates for the same period in consecutive years can be different by an order of magnitude or more (e.g. July 2006 vs.

July 2007), which seems unlikely. Precipitation in the summer period (June-August) is a potential factor, as precipitation totals are slightly different between years (14.42 cm, 24.43 cm, and 17.5 cm for 2006, 2007, and 2008, respectively). However, atmospheric heat flux, groundwater temperature, and stream temperature are also potential sources of error.

In 2006, the best-guess groundwater temperatures were up to 2 ˚C lower than in corresponding periods in 2007. To ensure that this was not a source of error, the simulations of 2006 were re-run using 2007 groundwater temperatures (not shown). The elevated groundwater temperatures increased the groundwater inflow rates by 60% on average, but did not produce the values seen in the 2007 simulations. The impact of atmospheric heat flux and stream temperatures on groundwater flow rate was investigated in a sensitivity analysis that is presented in the next section. The main conclusion of the analysis, as it applies to this particular stream reach, is that the discrepancy between the groundwater inflow rates predicted for the three years is due to opposite regimes in the stream temperature data between years, i.e. upstream-downstream temperature difference was positive in 2006, mostly negative in 2007, and positive in 2008. This contrasting behavior suggests inconsistency in how the temperature loggers were installed in each year, and means that simulations for this stream reach may have to be re-considered.

6.1.4. Reaches 4 and 5: Middle Main Stem of the Vermillion River

The model was applied to two consecutive sections of the middle Vermillion River: AES-58 to AES-56 (Reach 4), and AES-56 to AES-49 (Reach 5). Reach 4 had sufficient data to allow for application to both 2007 and 2008, while Reach 5 could only be analyzed for summer and fall of 2007 due to the loss of a temperature logger in 2008. Neither reach is particularly well-shaded; shading/sheltering was estimated to be 20% for the first reach and 30% for the second reach. Groundwater temperatures are taken from the analysis in Appendix B, with the exception of 2008 in which observed groundwater temperatures were used. Results are shown in Table 6.4 for Reach 4 and in Table 6.5 for Reach 5.

For Reach 4, mean groundwater contribution is 26% of observed stream flow for 2007 versus 47% for 2008, whereas the mean absolute groundwater inflow rates, while unnaturally large, are very similar in the two years (4.3 cfs/mile in 2007 and 4.7 cfs/mile in 2008), suggesting the presence of consistent, deep groundwater inflow in the reach. This is consistent with the conclusions of the EOR study, which identified this reach as a ‘strong raining reach.’ In 2007, results show a highly variable groundwater inflow to the Reach 4, with a range of 0.33 to 8.0 cfs/mile (6% to 44% of stream flow); in 2008, the range is 2.3 to 6.2 cfs/mile (12% to 83%). The higher percentages in 2008 are thought to be the result of lower stream flows, caused by the lack of precipitation and the diversion of wastewater treatment plant effluent upstream of this reach in March of 2008.

The simultaneous occurrence of large rainfalls and large stream flows, particularly in 2007, most likely indicates that significant tributary and surface inflows were present. These conditions are expected to result in over-predicted groundwater inflow rates and

are the likely cause of the many unrealistically high inflow values simulated for this reach.

Even higher groundwater inflow rates were calculated for Reach 5 (the downstream reach) than for Reach 4 (the upstream reach) for 2007. Values ranged from 5.1 to 11.1 cfs/mile (20% to 42% of stream flow), with a higher estimated mean inflow rate (7.2 cfs/mile) than in the upstream reach (4.3 cfs/mile). Again, the absolute values of groundwater inflow are unreasonably high. While the reach downstream of Empire is likely a groundwater-gaining reach, the presence of high stream flows and significant tributaries in the reach as well as the availability of only one year of data allow for only qualitative conclusions.

Table 6.4. Estimated (groundwater) inflow rate (Q_g) to a reach in the middle Vermillion River main stem (Reach 4; AES-58 to AES-56) in 2007 and 2008. Calculated from observations of stream flow, stream temperature and weather, and using a prescribed groundwater temperature (2007) or observed groundwater temperature (2008). Total precipitation and mean measured stream flow (Q_s) per period are also shown.

Period	Qs (cfs)	Precip (cm)	Tg (°C)	Qg (cfs/mi)	Qg (% Qs)
2007					
June 16-30	43.4	2.24	13	8.00	44
July 1-15	38.8	2.69	14	6.90	42
July 16-31	30.5	0.25	14	4.60	31
Aug 1-15	33.6	7.57	15	0.33	2
Aug 16-31	77.4	9.96	15	3.00	8
Sep 1-15	44.3	3.48	15	3.70	20
Sep 16-30	54.0	8.56	14	1.30	6
Oct 1-15	81.5	6.35	14	6.50	19
2008					
June 1-15	109	6.81	12.8	5.31	12
June 16-30	55.0	0.23	14.2	3.52	16
July 1-15	38.2	3.00	15.3	3.39	22
July 16-31	29.0	1.40	16.5	2.26	19
Aug 1-15	21.3	2.54	17.2	5.73	65
Aug 16-31	18.0	3.53	17.3	6.15	83
Sep 1-15	17.0	2.72	15.5	5.62	76
Sep 16-30	18.0	2.87	15.1	5.94	80

It is important to remember that the inflow rates estimated by the model are total inflow rates and can include surface water inflow from tributaries. Both reaches have significant tributaries, and carried more flow than baseflow during the second half of 2007. This may explain the relatively high inflow rates in the 2007 modeling period for both reaches, as heavy rains fell in August and September after a very dry summer period. While the tributaries may have been dry during the early summer, by late summer and early fall they would have contributed significant flows to the stream. This hypothesis is supported by the more consistent results for Reach 4 in 2008 (a consistently dry year) and the observation that periods of high flow and high rainfall occur simultaneously, i.e. without time lag. In North Creek and the upper main stem (Reach 3) a slight lag was observed.

Table 6.5. Estimated (groundwater) inflow rate (Q_g) to a reach in the middle Vermillion River main stem in 2007 (Reach 5; AES-56 to AES-49). Calculated from observations of stream flow, stream temperature and weather, and using a prescribed groundwater temperature. Total precipitation and mean measured stream flow (Q_s) per period are also shown.

Period	Qs (cfs)	Precip (cm)	Tg (°C)	Qg (cfs/mi)	Qg (% Qs)
2007					
June 16-30	76.2	2.24	13	9.1	42
July 1-15	66.4	2.69	14	7.7	41
July 16-31	50.5	0.25	14	5.5	39
Aug 1-15	52.0	7.57	15	5.1	34
Aug 16-31	117.0	9.96	15	11.1	35
Sep 1-15	72.0	3.48	15	7.7	37
Sep 16-30	72.5	8.56	14	5.1	23
Oct 1-15	105.0	6.35	14	6.5	20

6.1.5. Reach 6: Lower South Branch

The model was last applied to South Branch just upstream of its confluence with the Vermillion River main stem (AES-23 to AES-21). Data were available for fall 2006 and for summer-fall of 2007 and 2008. Groundwater temperatures as prescribed from the analysis in Appendix B were used for 2006 and 2007, and groundwater temperature data were used for 2008. Shading was estimated to be 66%. Results are shown in Table 6.6.

The results for lower South Branch are characteristic of a groundwater-fed stream that receives little surface runoff except during periods of rainfall: groundwater input is relatively constant for 2007 (0.60 to 1.50 cfs/mile, excluding a high-flow period in October that likely includes significant tributary inflow), and makes up a significant percentage of stream flow (25% to 63% in 2007), especially during dry periods. During periods of heavy rainfall (e.g. August 2007), stream flow increases by nearly an order of magnitude but groundwater inflow increases by only a factor of 2 or 3. These factors suggest that the groundwater input to South Branch is both significant and perhaps a combination of both shallow and deep groundwater.

The 2008 results for South Branch should be considered separately for two reasons. First, measured groundwater temperatures were used in 2008 in place of 'best-guess' groundwater temperatures because the data appeared to be good, but these values are considerably lower than those used in the 2006 and 2007 simulations. Second, the method of calculating discharge for the reach changed between 2007 and 2008, and the rating curve in 2008 was developed mainly from flows measured in that year. This explains the higher flows observed in 2008, which was a much drier year than 2007 and thus lower flows would be expected. In general, estimated groundwater inflow rates were similar between 2007 and 2008 (mean seasonal inflow of 1.02 cfs/mile in 2007 and 0.89 cfs/mile in 2008), though 2008 showed more variability, with a range of 0.2 to 1.64

cfs/mile. It is possible that the results for 2008 might be more representative of actual groundwater inflow for the reach given that it was a dry year, and the tributaries along the reach would be contributing very little flow.

Table 6.6. Estimated groundwater inflow rate (Q_g) to lower South Branch (Reach 6) in 2006 - 2008. Calculated from observations of stream flow, stream temperature and weather, and using a prescribed groundwater temperature. Total precipitation and mean measured stream flow (Q_s) per period are also shown.

Period	Qs (cfs)	Precip (cm)	Tg (°C)	Qg (cfs/mi)	Qg (% Qs)
2006					
Sep 16-30	10.8	1.36	12	0.86	22
Oct 1-15	15.2	0.41	11	0.41	8
Oct 16-31	13.8	0.10	11	1.60	32
2007					
June 2-15	10.8	1.7	13	1.20	33
June 16-30	6.4	2.24	13	0.81	37
July 1-15	4.1	2.69	14	0.84	58
July 16-31	2.7	0.25	14	0.60	63
Aug 1-15	6.2	7.57	15	0.6	38
Aug 16-31	18.9	9.96	15	1.3	25
Sep 1-15	10.7	3.48	15	1.3	34
Sep 16-30	15.3	8.56	14	1.5	28
Oct 1-15	22.6	6.35	13	2.7	34
2008					
June 1-15	30.7	6.81	9.7	1.64	15
June 16-30	18.5	0.23	9.6	1.64	26
July 1-15	11.8	3.00	9.9	1.43	34
July 16-31	9.1	1.40	10.1	0.87	27
Aug 1-15	7.6	2.54	10.1	0.6	22
Aug 16-31	5.8	3.53	10.2	0.5	23
Sep 1-15	6.0	2.72	10	0.3	13
Sep 16-30	7.1	2.87	10	0.2	8

6.1.6. Seasonal Averages of Estimated Groundwater Inflow

The estimated mean seasonal (June – September) groundwater inflow rates to each stream reach in 2007 and 2008 are shown in Figure 6.1. Results are presented both in cfs/mile and as the percentage of observed stream flow contributed by groundwater inflow in the modeled stream reach. All five stream reaches investigated are 'gaining' reaches with significant groundwater contributions (22% to 40% of streamflow in 2007 and 11 to 67% in 2008). The map in Figure 6.1 shows considerable spatial variation of groundwater inflows, which is related to both the hydrogeology of the watershed and to modeling errors at high stream flow.

The mean groundwater inflow rates are of similar magnitude in 2007 and 2008, despite different seasonal precipitation totals (36.5 cm in 2007 vs. 23.1 cm in 2008). In two of the

stream reaches (North Creek and the main stem upstream of the USGS gaging station), the estimated groundwater inflow rates were higher in the drier year; in two other stream reaches (South Branch and upper main stem reach) they were lower for the drier year. Possible explanations for the higher inflow in the drier year are: (1) the middle main stem reach appears to receive some groundwater from a deeper aquifer, as indicated by streambed temperatures that are consistently low throughout the year; (2) North Creek received a construction site de-watering discharge in 2008; and (3) lower stream stages create a larger head gradient between the water table and the stream, which may enhance groundwater inflow.

6.1.7. Summary of Results for Baseflow vs. High-Flow Conditions

In general, groundwater inflow to the Vermillion River varies considerably with location and with time. A comparison of simulation results from all modeled reaches for a single time period provides a picture of the spatial variability of groundwater inflow in the Vermillion River; repeating this exercise for two different flow conditions in the Vermillion River provides an illustration of the significant temporal variability of groundwater inflow.

First, a dry period (July 16-31, 2007) was selected for analysis in order to approximate baseflow conditions; results under these conditions are less likely to be influenced by tributary and shallow groundwater inflow. A map of the Vermillion River showing modeled stream reaches and estimated groundwater inflow rates for these reaches is shown in Figure 6.2. Groundwater inflow is given in values of cfs/mile, while the values in parentheses next to the stream gaging station markers are the stream flows as measured at those stations, averaged over the interval of analysis. The results indicate that during dry conditions, a significant amount of groundwater is coming in along the upper Vermillion main stem, and in the middle main stem near the USGS gaging station. Both South Branch and North Creek do not appear to contribute much groundwater during baseflow conditions. That the main stem reaches appear to contribute the most groundwater could be the result of significant tributary inflow along these reaches, in particular for the middle main stem where there are a number of tributaries, some of which may flow all summer.

Next, a relatively high-flow period was chosen in which significant rainfall had occurred in the previous month; September 1-15, 2007 was used due to the heavy rains that occurred in the watershed in August. It should also be noted that this period occurs roughly a month after the period used to approximate baseflow conditions (Figure 6.2), so a direct comparison of the results should provide insight into the impact of significant rainfall on groundwater input. Figure 6.2 also shows modeled reaches in the Vermillion River and their corresponding estimated groundwater inflow rates (cfs/mile) for September 1 – 15, 2007.

In general, inflow rates throughout the watershed are greater for the high-flow period than for baseflow conditions (the lone exception being the middle main stem upstream of the USGS station). Similar spatial variability as under baseflow conditions is present,

with the largest inflows again occurring in the upper and middle main stems of the Vermillion River. It should again be acknowledged that the presence of tributaries in these reaches may skew results, as any surface runoff or tributary contributions are lumped into the groundwater inflow by the model. The increase in groundwater inflow between periods is not uniform throughout the watershed; the largest increases (in percent) occurred in North Creek and in South Branch. In spite of the presence of tributaries, it is likely safe to assume that shallow groundwater contribution is especially significant in the lower portion of the watershed (middle main stem of the Vermillion River and South Branch), and underscores the fact that spatial and temporal variability of groundwater inflow to the river makes it a very difficult parameter to estimate accurately.

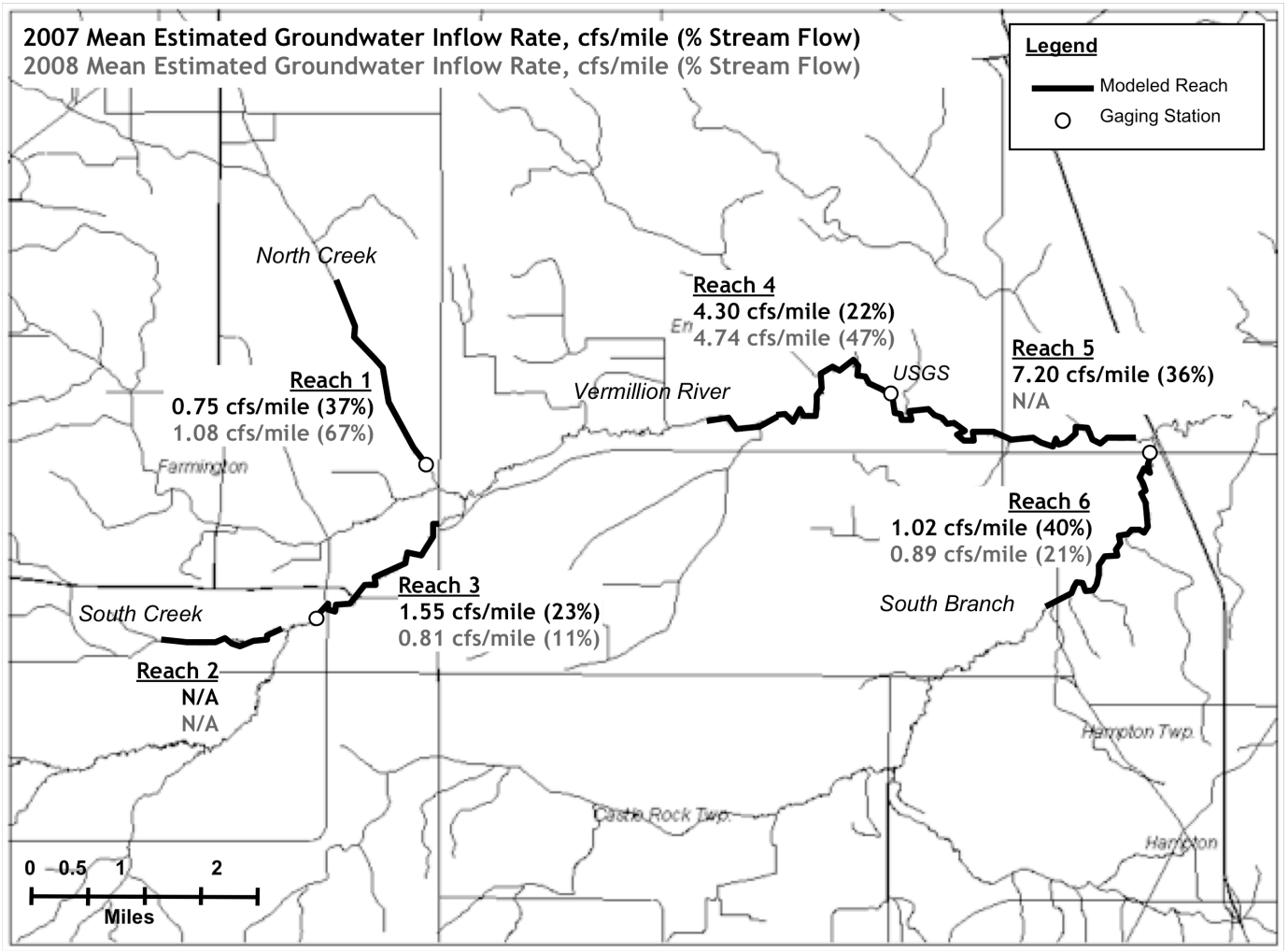

Figure 6.1. Estimated mean seasonal groundwater inflow rates (cfs/mile) into five modeled stream reaches for June – September, 2007 (black), a relatively wet summer, and for June – September, 2008 (gray), a very dry summer. Values in parentheses give the percentage of observed stream flow at the downstream end of each reach that is contributed by the modeled groundwater input in that reach. Note that South Creek was not modeled due to lack of data.

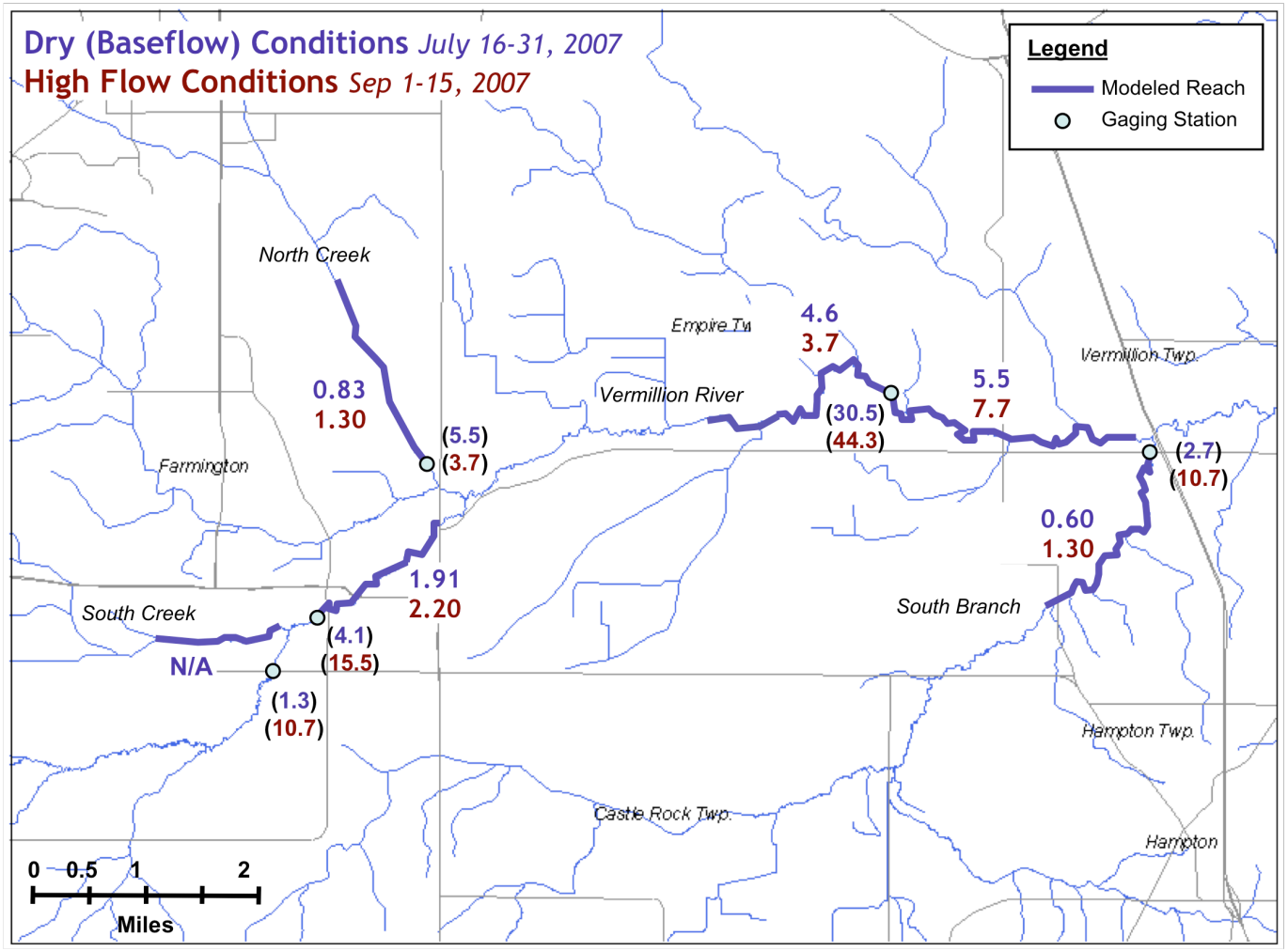

Figure 6.2. Map of modeled reaches in the Vermillion River and major tributaries. Mean estimated groundwater inflow rates in units of cfs/mile are shown for July 16-31, 2007 (blue), a dry period corresponding to baseflow conditions, and for Sep 1-15, 2007 (red), a relatively high-flow period occurring after heavy rains in August. Values in parentheses next to gaging station markers are measured stream flows (in cfs) at those sites, averaged over the same periods as the groundwater values. Note that South Creek was not modeled for this period due to lack of data.

6.2. Sensitivity of Predicted Groundwater Inflow Rates

6.2.1. Sensitivity to groundwater temperature and stream shading/sheltering

Given the uncertainty in determining groundwater temperature and shading/sheltering for a stream reach, a sensitivity analysis was performed to assess the impact of these two parameters on estimated groundwater inflow rate. Since the heat flux contributed by groundwater to a stream is the product of groundwater flow rate and groundwater temperature (Equation 2), modification of groundwater temperature will have a direct effect on estimated groundwater inflow rate. Similarly, since atmospheric heat flux is the largest heat contribution to a stream (particularly during daylight hours), shading and sheltering will have a direct effect on the amount of solar radiation reaching the stream and the effective wind speed at the water surface, respectively. As in the case of the simulations conducted previously, shading and sheltering are assumed to be essentially equal.

For the sensitivity analysis, groundwater inflow rates were computed for selected intervals on the upper Vermillion River main stem (Reach 3) for a range of groundwater temperatures and shading/sheltering coefficients. Time periods in which little or no rainfall occurred were simulated in order to minimize the effect of storm water inflow. Groundwater temperature was varied in 1˚C increments over a 6˚C range (i.e. 8 – 14 ˚C), while four shading/sheltering values were used (0%, 45%, 70%, and 95%).

Results are shown in Table 6.7 for the week of July 1-7, 2007. This was a period of low stream flow (5.6 cfs), though some rainfall occurred (1.5 cm). Groundwater temperature was varied from 8 ˚C to 14 ˚C.

Table 6.7. Estimated groundwater inflow rate (cfs/mile) to the upper main stem of the Vermillion River (Reach 3; AES-79 to CHP-1) for July 1-7, 2007, as a function of groundwater temperature (T_g) and shading/sheltering coefficient (SH). Mean stream flow is 5.6 cfs, reach length is 2 miles.

Tg (˚C)	SH = 0.0	SH = 0.45	SH = 0.70	SH = 0.95
8	2.29	1.85	1.11	0.448
9	2.34	2.02	1.27	0.564
10	2.45	2.2	1.57	0.711
11	2.6	2.34	1.87	0.878
12	2.72	2.53	2.15	1.1
13	2.72	2.72	2.36	1.47
14	2.72	2.72	2.55	1.94

For this period both groundwater temperature and shading coefficient appear to have a significant effect on predicted groundwater inflow rate, though the effect is not uniform. For example, decreasing shading from 95% to 0% increases groundwater inflow rate by as much as 400% (e.g. for T_g = 8 ˚C or 9 ˚C). The effect of increasing groundwater temperature (T_g) appears to be highly dependent on shading: increasing T_g from 8 ˚C to

14 ˚C for 0% shading leads to very little increase in groundwater inflow rate, while for 95% shading the same increase results in a four-fold increase in groundwater inflow rate. This result is logical, since in the case of near complete shading very little atmospheric heat flux is reaching the stream, and stream temperature is considerably more sensitive to groundwater input. By contrast, for the no-shading case the stream temperature dynamics are driven almost completely by atmospheric forcing, and groundwater plays a small role.

These sensitivity simulations were repeated for the week of September 8-14, 2007, which was a dry, moderate-flow period (no rainfall, 16.7 cfs mean stream flow). Groundwater temperature was varied from 9 ˚C to 15 ˚C. Results are shown in Table 6.8.

Table 6.8. Estimated groundwater inflow rate (cfs/mile) to the upper main stem of the Vermillion River (Reach 3; AES-79 to CHP-1) for September 8-14, 2007, as a function of groundwater temperature (T_g) and shading/sheltering coefficient (SH). Mean stream flow is 16.7 cfs, reach length is 2 miles.

Tg (˚C)	SH = 0.0	SH = 0.45	SH = 0.70	SH = 0.95
9	2.19	0.472	0.117	0.117
10	3.64	1.24	0.284	0.117
11	4.87	2.65	1.84	1.22
12	6.56	4.09	2.06	2.26
13	7.08	5.1	3.39	3.07
14	6.95	5.41	4.52	4.82
15	5.9	5.46	4.6	5.37

The effect of groundwater temperature and shading/sheltering on predicted groundwater inflow rate for this early-September period is considerably bigger than for the July period. For example, for a groundwater temperature of 11 ˚C, the estimated groundwater inflow rate for a no-shading case is 4 times higher than that predicted for 95% shading; the effect is less for higher groundwater temperatures. For lower groundwater temperature, the results can be misleading, as it appears that for T_g = 10 ˚C, the no-shading scenario results in a groundwater inflow rate that is 30 times higher than for the 95% shading scenario. However, due to rounding errors in the iteration procedure of the model, the groundwater inflow rate can never be zero, and the 0.117 cfs/mile value in the table is essentially zero groundwater inflow.

As shown previously, the extent to which groundwater temperature influences groundwater inflow rate is dependent on the level of stream shading; a greater effect occurs for higher shading levels. This is consistent with the fact that stream temperature dynamics are atmosphere-dominated for low shading values and groundwater-dominated for high shading values, which explains the greater sensitivity to groundwater temperature at high shading values.

It should also be noted that in the zero-shading case, the peak estimated groundwater inflow rate occurs at 13 ˚C rather than at 15 ˚C, as it does for the other shading levels. This is likely the result of the fact that mean stream temperature over this interval is 13.1˚C, which would lead to a large groundwater inflow rate due to the very small

temperature difference between the stream and groundwater. That the other shading levels do not show a maximum inflow rate at T_g = 13 ˚C and instead increase very slightly for groundwater temperatures higher than 13 ˚C is likely the result of the greater influence of groundwater temperature for these shading levels relative to the no-shading case.

6.2.2. Sensitivity to atmospheric forcing, stream temperatures, and stream flow

An additional analysis was performed to correlate model output (groundwater inflow to the stream) with parameters specified by input data (stream temperature and atmospheric heat flux) as opposed to user-specified parameters (groundwater temperature and shading/sheltering). Reach 3 (upper Vermillion River main stem) was used for most of this analysis as it had a longer data record and slightly more consistent results than the other two sites.

For the first part of this analysis, time-averaged net atmospheric heat flux was computed for each simulation period using mean observed stream temperatures and then compared with the estimated groundwater inflow rates for the same periods. In general, very little correlation was found between atmospheric heat exchange and groundwater inflow rate for any of the reaches (R^2 = 0.009 to 0.34 for a linear fit). Since there is no physical basis for a relationship between these two quantities, this result is encouraging.

In the second part of this analysis, mean upstream-downstream temperature difference for each simulation period was calculated. A positive value indicates an increase in temperature along the reach (i.e. a ‘warming’ reach). In calculating the upstream-downstream temperature difference, the downstream temperature was lagged by the travel time of the stream in an attempt to estimate the change in temperature of a parcel of water as it travels along the reach (the main principle of Model 2). In general, no strong trends were present in any of the reaches (R^2 = 0.06 to 0.25), although the higher groundwater inflow rates occurred in ‘cooling’ reaches, while smaller groundwater inflow rates occurred in ‘warming’ reaches (results not shown). This suggests that a stream-wise water temperature gradient in a reach, taken alone, may not be a good indicator of the amount of groundwater inflow.

Closer inspection of atmospheric and stream temperature quantities can reveal the sources of discrepancy in predicted groundwater inflow rates between years. For example, consider the upper Vermillion River reach (Reach 3) in 2006 and 2007 (Table 6.9). For the summer periods (June – August), the mean upstream-downstream temperature difference is positive in 2006 but negative in 2007, meaning that a net loss of heat is occurring for water as it moves along the reach in 2007. As groundwater nearly always has a cooling effect on a stream, a negative difference in stream temperature means that more groundwater is required to achieve the cooling effect, and therefore the computed groundwater inflow rate will be higher than in the case where a heating effect is being observed. In terms of net atmospheric heat flux, the values are slightly higher in 2006 than in 2007, which helps account for the model predicting any groundwater inflow

rate at all in 2006, given that stream temperature is increasing along the length of the reach.

Table 6.9. Estimated groundwater inflow rate (Qg) to the upper Vermillion River (Reach 3; AES-79 to CHP-1) in 2006 and 2007, along with time-averaged net atmospheric heat flux and mean upstream-downstream temperature difference.

Period	Qs (cfs)	Qg (cfs/mi)	Qg (% Qs)	Mean ΔT (°C)	Mean Atm (W/m^2)
2006					
June 1-15	15.2	0.16	2	0.92	31
June 16-30	20.8	0.26	2	0.39	33
July 1-15	13.2	0.14	2	0.67	56
July 16-31	11.5	0.18	3	0.80	65
Aug 1-15	22.8	0.29	3	0.61	20
Aug 16-31	13.6	0.26	4	0.57	7
2007					
June 1-15	11.7	0.15	3	0.45	25
June 16-30	9.3	1.19	19	-0.44	29
July 1-15	5.3	2.12	44	-1.66	19
July 16-31	4.1	1.91	49	-2.37	14
Aug 1-15	8.7	1.12	29	-1.34	7
Aug 16-31	29.9	0.90	6	0.45	-42
Sep 1-15	19.9	2.20	17	0.72	-26
Sep 16-30	20.0	2.80	19	0.65	-33
Oct 1-15	27.3	3.87	20	0.24	-84

While the results in Table 6.9 show that the magnitude of the estimated groundwater inflow rate in Reach 3 has a slight dependence on observed stream temperatures between the upstream and downstream ends of the stream reach, they do not indicate if the measured stream temperature data are faulty or not. However, the opposite trends in the data from the two years suggest that the stations were not installed consistently between years in this particular reach.

Groundwater inflow rates were also related to the stream temperature-groundwater temperature difference (T_s-T_g) for every simulation period in each reach. While decreasing trends are present in plots of groundwater inflow rate versus T_s-T_g for all reaches, the strongest trends are present in the upper Vermillion River reach (Reach 2) and the middle main stem reach (Reach 3). A linear relationship fitted the data for these two sites with $R^2 = 0.57$ and $R^2 = 0.75$, respectively (Figure 6.3). These trends indicate that, as expected, the model will not give reliable groundwater inflow estimates as groundwater temperature approaches the stream temperature: a smaller temperature difference between the stream and the groundwater requires more groundwater to 'maintain' the observed stream temperatures. The predicted inflows will then be unrealistically large. This condition also underscores the need for accurate water temperature measurements.

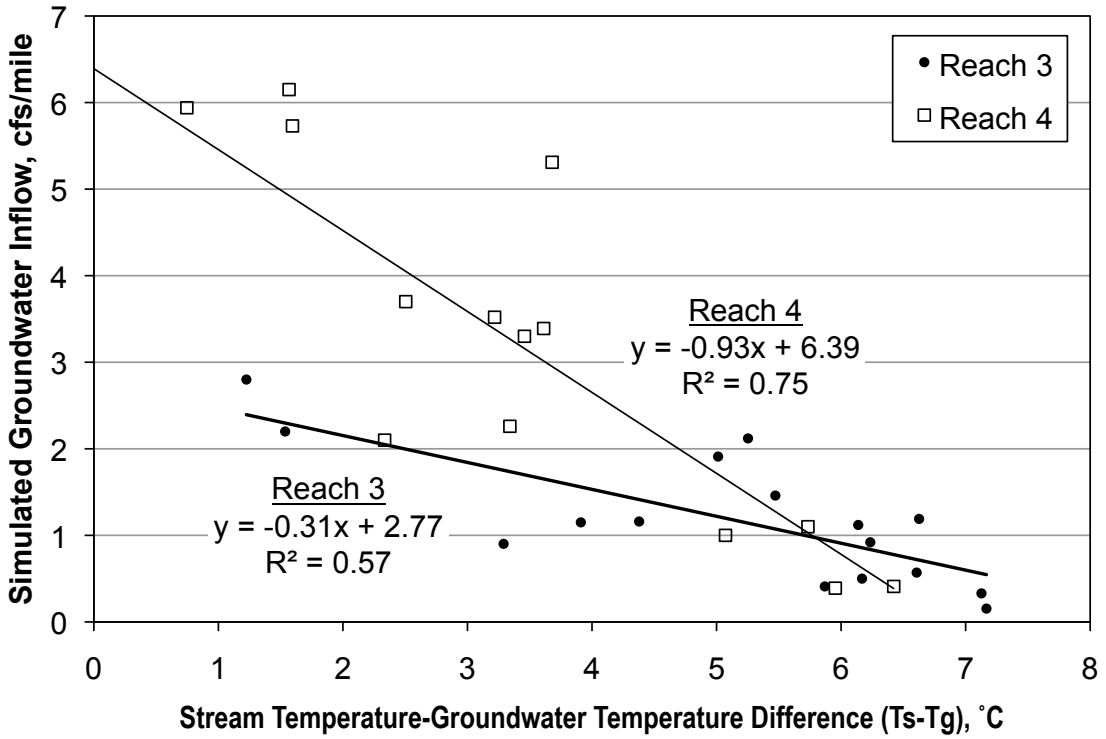

Figure 6.3. Simulated groundwater inflow in cfs/mile vs. mean stream temperature - groundwater temperature difference (Ts-Tg) in ˚C for the upper Vermillion River main stem (Reach 3) and for the middle Vermillion River main stem (Reach 4) for the 2007 and 2008 simulation periods. Linear fits shown.

Sensitivity to stream flow was also tested. The model was not expected to perform well for periods of high flow, primarily for two reasons: (1) surface inflows, when present, are lumped into the groundwater inflow by the model and consequently lead to over-predicted inflow rates, and (2) groundwater will comprise a smaller portion of the overall flow as stream flow increases, meaning its contribution to the heat budget should be harder to detect accurately. Furthermore, the residual of the stream heat budget (from which groundwater inflow is calculated) becomes larger as stream flow increases since even small changes in stream temperature represent large amounts of heat, leading also to over-predicted groundwater inflow rates. This expectation was confirmed by the discovery of a relationship between the modeled groundwater inflow and the observed stream flow ($R^2 = 0.56$ for a linear fit) for flows higher than about 20 cfs (Figure 6.4). Above this point, groundwater inflow rates generally exceeded 2 cfs/mile, which is already an unreasonably high groundwater inflow rate for the Vermillion River stream system. In other words, the groundwater model is systematically over-predicting groundwater inflow rates for stream flows greater than 20 cfs.

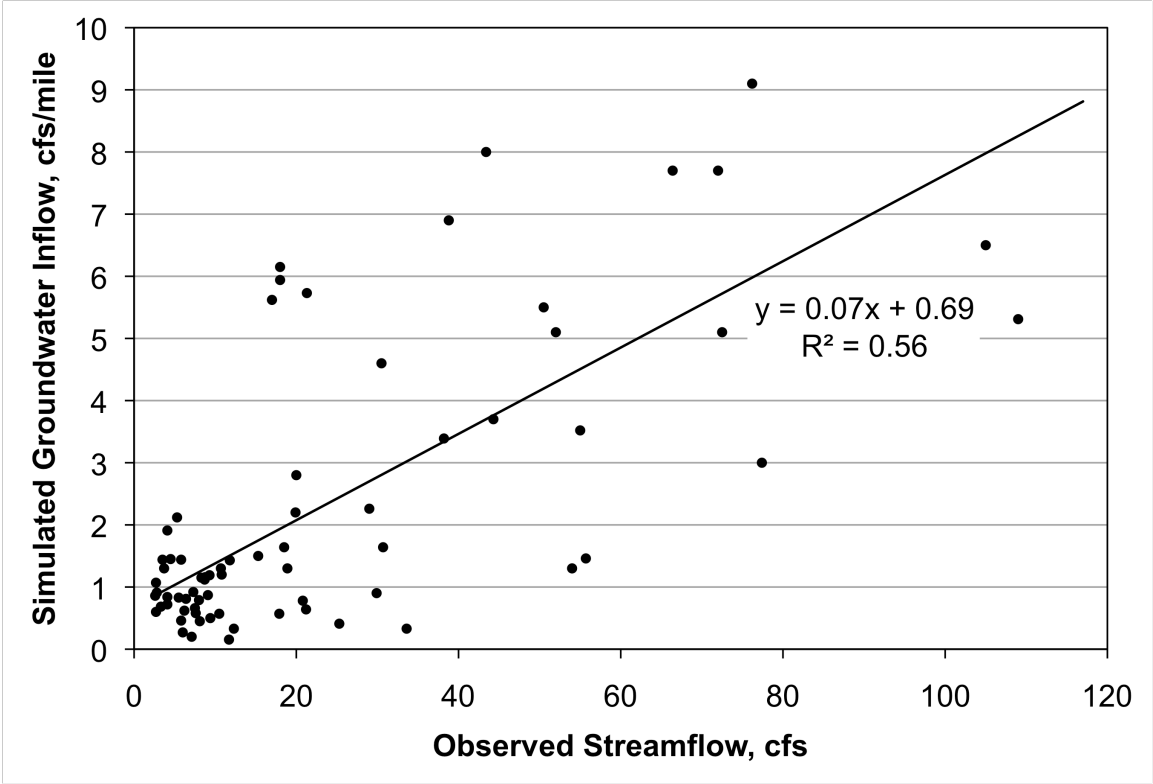

Figure 6.4. Simulated groundwater inflow (cfs/mile) vs. mean observed stream flow (cfs) for all sites for the 2007 and 2008 simulation periods. Linear fit shown.

In the case study there were periods of significant rainfall, most notably August-September of 2007 and June 2008. Omission of these periods had a slight impact on the seasonal averages of groundwater inflow rate for most of the modeled reaches (Table 6.10), generally causing the predicted inflow rates to decrease by 11-16%. Slightly larger decreases logically occurred in the wetter year (2007) compared to the drier year (2008). A couple of exceptions should be noted, however. Inflow rates in North Creek increased slightly in 2008 with the omission of wet periods, which could be related to the more pronounced impact of construction dewatering at low flows. Similarly, in Reach 3, the estimated groundwater inflow rate increased by 50% in 2007 and remained largely unchanged in 2008 when wet periods were omitted; the cause of the increase in 2007 is not apparent, especially when a decrease would have been expected.

Table 6.10. Simulated groundwater inflow rates (cfs/mile) by reach and by year. Values shown are summer averages including all simulation periods for which data were available, and neglecting periods in which significant rainfall occurred (August – September 2007, and early June 2008).

Reach Name (Number)	2007			2008		
	All Periods (cfs/mile)	Dry Periods (cfs/mile)	% Change	All Periods (cfs/mile)	Dry Periods (cfs/mile)	% Change
North Creek (1)	0.75	0.63	-16%	1.08	1.14	6%
Upper Main Stem (3)	1.55	1.34	-13%	0.81	0.72	-11%
Middle Main Stem, Upstream USGS (4)	4.29	6.50	51%	4.74	4.66	-2%
Middle Main Stem, Downstream USGS (5)	7.50	7.50	0%	n/a	n/a	n/a
South Branch (6)	1.02	0.86	-16%	0.89	0.78	-12%

6.3. Correlation with Hydrologic Parameters (Precipitation and Stream Stage)

Groundwater input to a stream, particularly in a watershed that has a shallow aquifer with a high transmissivity, will be influenced by stream level and antecedent precipitation. This is because groundwater inflow is driven by a difference in water level between the water table and the stream. Water flows down this gradient, generally at a rate proportional to the groundwater transmissivity of the soil. We don't have data available to tell us the groundwater level near the stream, but the source of this water is primarily infiltrated rainfall; thus precipitation, along with stream stage, is likely to determine the amount of groundwater inflow to a stream.

We therefore conducted a multiple linear regression analysis to investigate the correlation of estimated groundwater inflow rate to stream stage and antecedent rainfall. Precipitation was summed into bins of increasing size (0.5 month, 1 month, 1.5 months, and 2 months) and was lagged behind estimated groundwater inflow rate and stream stage by varying amounts (0.5 month, 1 month, 1.5 months). This was an attempt to take into account the time required for rainfall infiltrated in previous months to make its way to the stream ('time of concentration'), which is an unknown but relatively short amount of time in this watershed.

The analysis was applied to reaches in which in which simulations had been run for both 2007 and 2008: North Creek, the upper main stem of the Vermillion River (VR807 to CHP-1), the reach upstream of the USGS station on the middle main stem (AES-58 to AES-56), and South Branch. The results varied considerably between reaches (see Table 6.11). Also of note is that variation in the lag time between precipitation and groundwater inflow was found to have little effect on the results, and thus results are presented for the zero lag case only.

Table 6.11. Multiple linear regression results for comparison of simulated groundwater inflow rate to measured stream stage and antecedent precipitation for 2007 and 2008. 'Precipitation Bin Size' is the length of period over which precipitation was totaled. Flow rate was used instead of stage on South Branch due to the changes in how stage was measured at that site between 2007 and 2008.

Reach	Precipitation Bin Size			
	0.5 mo.	1.0 mos.	1.5 mos.	2 mos.
North Creek	0.13	0.09	0.08	0.08
Upper VR	0.23	0.4	0.74	0.63
Middle VR	0.21	0.18	0.22	0.34
South Branch	0.62	0.61	0.63	0.64

In North Creek, very little correlation was found between estimated groundwater inflow rate and precipitation and stream stage. That the smallest bin size coupled with 0-lag had the 'highest' correlation is a clue that this particular area of the watershed responds quickly to inputs of precipitation. North Creek is known to be a 'flashy' system due to a high water table, sandy soils, and high amount of impervious surface area in its drainage basin. An analysis involving smaller precipitation bins might yield better results, but it is likely that relatively little rainfall infiltrates in this watershed and instead reaches the stream as surface runoff. Thus little correlation would be expected between groundwater inflow and precipitation.

For the upper Vermillion River main stem reach, a bin size of 1.5 months produced the highest correlation. The R^2 tended to increase with increasing bin size up to 1.5 months, and decrease slightly with increased lag (not shown). This suggests that the drainage area for this reach has a relatively high time of concentration (1.5 to 2 months) for shallow groundwater.

Very little correlation appears to exist between groundwater inflow rate and precipitation/stream stage for the middle main stem reach of the Vermillion River. It is not clear why this might be the case, but much as in the upper main stem reach, the time of concentration for groundwater appears to be relatively high (2 months). The large number of tributaries present in this reach will tend to introduce some error to the simulation results, and may help to explain the poor correlation results.

South Branch was the last analyzed reach. The R^2 values were surprisingly consistent (0.61 – 0.75 for all scenarios investigated) and did not depend on bin size, and generally tended to increase with increased lag (not shown). The case of a half-month bin with 1-month lag had the highest R^2 (0.75), but not by much, and therefore might not be significant. With such little differentiation between the various scenarios it is hard to make any definite conclusions, but it appears that some lag exists between precipitation and estimated groundwater inflow. This may be the result of a number of factors. First, this stream drains an area that is primarily agricultural, and the drainage tile system might serve to rapidly shunt water to the stream once it has infiltrated through the topsoil layer above the tile. However, this process probably occurs on a shorter time scale than the 2- or 4-week lag that gives the best results in this analysis. Other possible factors include the

presence of irrigation, which could provide a baseline groundwater inflow that fluctuates inversely with precipitation totals, or the presence of a deeper aquifer providing a substantial (but seasonally variable) amount of water to the system. It should also be pointed out that stream flow rather than stream stage was used for this reach because of the change in datum used to determine stream flow between 2007 and 2008 that prevented the calculation of stream depth in 2008.

It is acknowledged that this was not a rigorous statistical analysis, but the intention was to make some general observations in regard to correlation of groundwater inflow rate to hydrologic parameters (precipitation, stream stage) that would be expected to influence it in this watershed.

6.4. Comparison with Other Observed Flow Rates

Single stream flow measurements were taken at a number of points in the watershed as part of unrelated monitoring efforts by the Metropolitan Council and the Dakota County Soil and Water Conservation District. These measurements were made over a period of three days (September 4 – 6, 2007), both in the Vermillion River main stem and in major tributaries, including South Branch (Figure 6.5). A few of these measurements are located in or just upstream of modeled reaches, and while there are not enough data to provide a rigorous validation of the model, the data can provide a method to assess the general accuracy of the results.

These measured flow rates were compared to modeled flow rates by making a crude assumption that the groundwater inflow rates calculated for the reaches for the period of interest were valid even upstream of the reaches to the points where the additional flow measurements were made. An estimate of the flow rate upstream of the reach was thus made by subtracting the groundwater inflow (in cfs/mile * distance in miles) along the entire distance from the stream gaging site in the modeled reach up to the location of the point measurement. In South Branch, for example, the modeled reach was 2.8 miles long with the SB802 gaging station at the downstream end. For a point 1.6 miles upstream of the reach, groundwater inflow as calculated for the 2.8-mile reach was assumed to hold true up to the 4.4-mile mark for the sake of comparison. Results are summarized in Table 6.12 below.

6.4.1. South Branch

In South Branch, flow measurements were taken at two locations upstream of the modeled reach on September 5, 2007: one at Highway 50 (roughly 1.6 miles upstream of the modeled reach) and one at Blaine Avenue (about 3 miles upstream). Stream flows of 5.27cfs and 2.59cfs were measured at the two sites, respectively. Using the period average groundwater inflow rate (1.30 cfs/mile for September 1-15), flow was estimated to be 4.44 cfs and 2.66 cfs at Hwy 50 and Blaine Ave, respectively, resulting in an error of 16% and 3% for the two sites. While just a single point in time, these results are encouraging and suggest that for this reach the model does a fair job of estimating groundwater inflow to the stream.

6.4.2. Middle Main Stem of the Vermillion River

A total of three flow measurements were made in the middle reach of the Vermillion River main stem. One measurement was made a few miles upstream of the USGS gaging station near the Empire Wastewater Treatment Plant inflow on Sep 4 (41.0 cfs), and two measurements were made downstream of the station on Sep 5: one at Clayton Avenue (37.9 cfs) and the other a couple miles further downstream at Donnelly Avenue (42.3 cfs).

Unfortunately, the flow measured at Clayton Avenue was significantly lower than the 42 cfs recorded at the USGS station approximately one mile upstream of the site, which would indicate that the reach is a losing reach and not a significant gaining reach as shown by the model results (see Table 6.5 for Site #5). The measurement at Donnelly Avenue is about the same as the USGS value for the day, indicating a neutral reach. However, it is possible that some error exists in the point measurements or in the rating curve used by the USGS, and the apparent discrepancy in measured flows could also be attributed to differences in methodology. If taken separately from the USGS flow data, the measurements indicate that the downstream reach is likely a gaining reach: stream flow increases by 4.4 cfs over the two-mile distance between Clayton Avenue and Donnelly Avenue (2.2 cfs/mile), which is about 30% of the modeled value for the time period.

The results are slightly more encouraging for the measurement upstream of the USGS station. The estimated groundwater inflow rate for the reach (Site #4) for Sep 1-15, 2007 was 3.70 cfs/mile; when applied to the flow value recorded at the USGS station for Sep 4 (45 cfs), the estimated flow rate near the Empire WWTP outflow is 35 cfs, or about 85% of the measured flow at that point (41.0 cfs).

6.4.3. Middle Main Stem of the Vermillion River

A flow measurement was made on Sep 5 at the Chippendale Avenue bridge over the upper main stem of the Vermillion River, which also happens to be where the CHP-1 stream and groundwater temperature monitoring station is located on the downstream end of the modeled reach (Site #3). Using the period average of groundwater inflow for the reach (2.20 cfs/mile) and the measured flow at the VR807 station at the upstream end of the reach (12.7 cfs), a flow of 17.1 cfs is predicted at the CHP-1 station. This is roughly 25% higher than the observed flow of 13.7 cfs at CHP-1. Again, while the model does not match the observed flows perfectly, the results are encouraging.

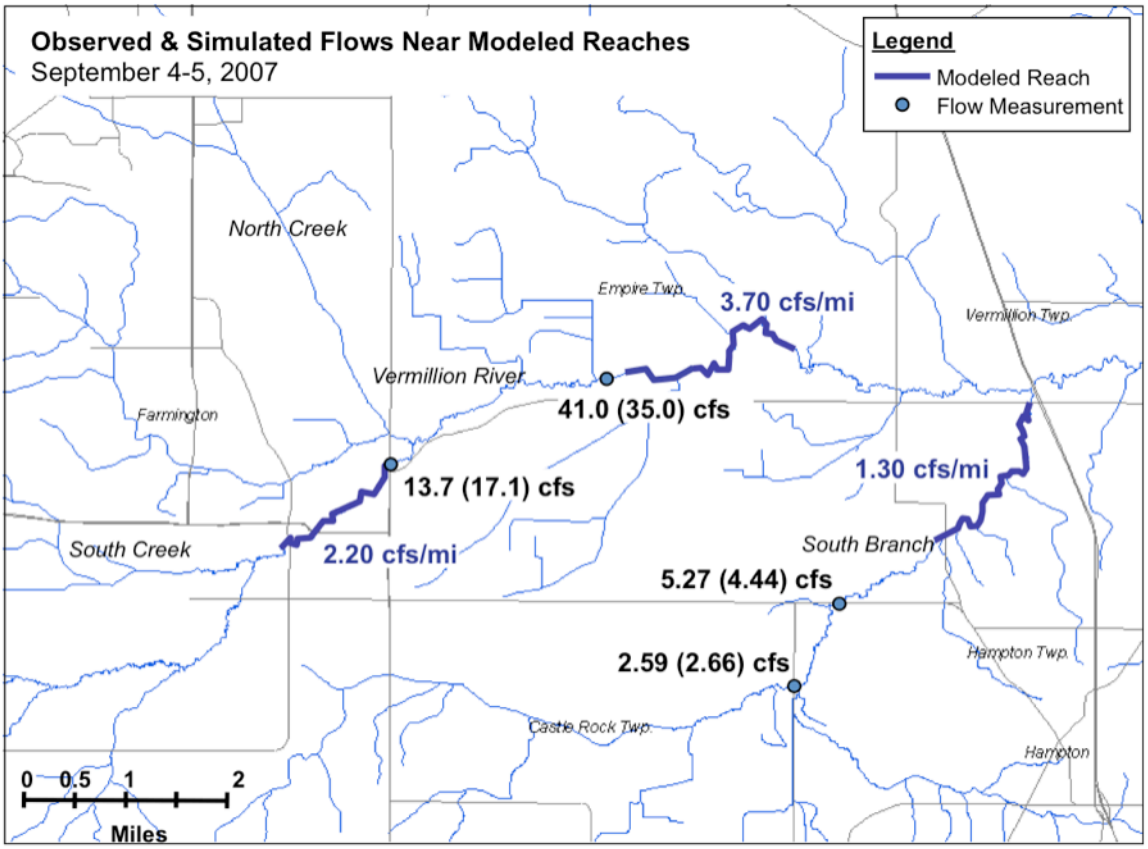

Figure 6.5. Location of single flow measurements taken Sep 4-5, 2007 near or in modeled reaches. Observed flows (cfs) are shown, with estimated flows in parentheses. Estimated flows are determined from gauged streamflows and modeled groundwater inflows (cfs/mi) in modeled reaches, the latter of which are also shown.

Table 6.12. Estimated and observed flow rates at points near modeled reaches for Sep 4-5, 2007. Location of point measurements and closest modeled reach is shown. Q,obs is the flow measured at that point in cfs, Q,est is the flow (in cfs) estimated at that point by using the modeled groundwater inflow rate and the flow recorded at a gaging station somewhere in the modeled reach.

Site	Nearest Reach	Location*	Q, obs (cfs)	GW Inflow (cfs/mile)**	Q, est (cfs)	Error
Hwy 50	South Branch	1.6 mi upstream	5.27	1.3	4.44	**16%**
Blaine Ave	South Branch	3.0 mi upstream	2.59	1.3	2.66	**3%**
Empire WWTP	Middle VR Main Stem	0.4 mi upstream	41	3.7	35	**15%**
Chippendale Ave	Upper VR Main Stem	downstream end	13.7	2.2	17.1	**25%**

* location relative to modeled reach (column 2)
** modeled groundwater inflow for the reach in column 2 for the Sep 1-15, 2007 period

7. Data Needs for Additional Model Application

The extent to which the model could be applied to the Vermillion River and its tributaries was limited. This is due primarily to two inter-related issues that made the model application difficult: (1) lack of favorable reaches for application of the model (i.e. spatial resolution of data), and (2) issues with data quality and availability. These issues are addressed here in order to provide insight for future monitoring efforts in the watershed.

7.1. Locations of stream temperature and gaging stations

The model requires that certain data and conditions are met for its application to specific stream reaches: stream temperature at the upstream and downstream ends of the stream reach, flow measurements at either end, and a minimal number of tributaries entering the reach. A so-called 'favorable' stream reach for model application is one in which all of these conditions are met.

While a large number of stream temperature stations are located in the Vermillion River watershed, the general strategy employed in their placement was not optimal for application of the model. In general they seemed to be placed downstream of all major confluences along the main stem and at the upstream and downstream ends of major tributaries. While this strategy was favorable for the tributaries, which did not have a large number of additional inflow points, on the main stem of the Vermillion River it was unfavorable. Additional stations placed upstream of major confluences would have been very useful.

Flow data were collected at several locations in the Vermillion River main stem, and in a few of the major tributaries (North Creek, Middle Creek, South Branch). In general the location of these stream gaging stations and the data obtained was favorable, although an additional station on South Creek and one on the main stem between the North Creek confluence and the USGS station were sorely missed. This situation can be remedied with placement of additional stream temperature stations along the main stem, and perhaps additional stream gaging stations.

7.2. Data quality

A number of difficulties were encountered in the use of the data, particularly groundwater temperature and stream temperature data. As was illustrated in the sensitivity analysis, stream temperature records sometimes showed inconsistent trends in consecutive years, such as the reversal of the upstream-downstream temperature difference in the upper Vermillion River reach from 2006 to 2007. Similarly, the data for South Creek showed that stream temperature increased significantly along this reach, which limited the model to a negligible groundwater input prediction for the reach, contrary to EOR's designation of the reach as 'groundwater gaining' (2007). These trends are not necessarily indicative of improper installations or faulty devices, and might instead be the product of a whole host of factors including proximity of stations to natural springs, changes in groundwater

or stream flow regime, channel modification, or weather conditions (drought, floods, heat, etc.)

Furthermore, it has to be acknowledged that trying to place a single temperature probe in a groundwater fed stream such that it measures the mean or characteristic temperature of the stream at that location is a difficult task. If placed too near the surface, it will read artificially high temperatures, especially on sunny days. If placed too near the streambed or shore it might be measuring an artificially low temperature closer to that of groundwater, at least if it is a gaining reach. This problem is exacerbated further if the probe is removed for the winter; even with GPS it is unlikely that the probe will be placed in the exact same location as the previous season. In light of this, it appears as if some of the stream temperature data suffers from inconsistent placement of probes between years or between data dumps.

In terms of groundwater temperature data, a significant amount of the data was unusable or had to be considered very carefully. This was due primarily to two factors: (1) improper installations at a number of sites in 2007 in which the temperature probe was not placed in the screened portion of the piezometer tube, and (2) a phenomenon in which the water in the tube began to mix vertically on a diurnal basis in the fall, leading to fluctuations in groundwater temperature. Due to accuracy concerns the data could not serve as a direct input for the model for 2007. Instead the groundwater temperature had to be specified, with the data used to help provide a best-guess estimate. A more detailed analysis of the groundwater temperature data is presented in Appendix B.

In 2008, the groundwater piezometers were installed with greater care and the devices modified to prevent diurnal mixing within the piezometer tubes. Thus for the 2008 simulations the groundwater temperature data was used directly, as it appeared to be of better quality than previous years. For most reaches the 2008 observed groundwater temperatures were slightly lower than those used in corresponding periods in 2006 or 2007; for South Branch this difference was considerable (around 3˚C or 4˚C) and should be taken into account when comparing the results between years. In this reach especially it appears as if the piezometers were placed in areas influenced heavily by spring inflow or deep groundwater.

7.3. Current and Future Reaches for Model Application

With the given locations of stream temperature and gaging stations, the model could only be effectively applied to seven reaches: North Creek, Middle Creek, South Creek, South Branch, the upper Vermillion River between the confluences with South Creek and with North Creek, and the middle main stem both upstream and downstream of the USGS gaging station. The six reaches that have been modeled thus far were chosen because they were known groundwater-gaining reaches and/or designated trout stream reaches, and had enough data available to run the model.

At this time there are no plans to apply the model to Middle Creek, as it is not a designated trout stream and does not contribute as much flow to the system as North

Creek. Additional reaches of the Vermillion River can also be modeled in the future if suitable data can be identified.

8. Summary and Conclusions

A model has been developed for estimation of groundwater inflow to a stream reach from observations of stream temperature, groundwater temperature, stream flow rate, and standard weather parameters. The purpose of this model is two-fold: (1) to provide an estimate of groundwater inflow rate for stream reaches that will be analyzed with more comprehensive models of stream temperature or other water quality parameters, and (2) to identify reaches where groundwater inflow is significant, which will be useful for fisheries managers and those managing development in urbanizing watersheds where stream temperature is a concern. In particular, the model was developed for use in the Vermillion River watershed, which contains designated trout reaches that have the potential to be impacted by development in the watershed.

The method of analysis was developed with the assumption that certain conditions and data were present: stream temperature at the upstream and downstream ends of a stream reach, stream flow at either end of the reach, standard weather data, and no significant tributaries or inflows between the ends of the reach. This limited the number of potential sites to roughly six on the Vermillion River and its tributaries. A summary of available data is given in Appendix A.

Additional factors have to be taken into account in the application of the method of analysis. First, the method must be applied to stream reaches where groundwater input is expected to be significant relative to the stream flow in order to ensure that the computed flow rates are greater than those resulting from the errors inherent in the input data. Since the groundwater inflow rate is computed from a stream heat budget, the model must be applied during time periods when a significant difference exists between stream temperature and groundwater temperature. If stream temperature and groundwater temperature are nearly identical, it becomes impossible to determine how much groundwater is present since it will not appreciably change stream temperature, even for a large groundwater flow.

8.1. Simulation Results

The model was applied to six reaches in the Vermillion River watershed, including North Creek, South Creek, South Branch, the upper Vermillion River between the confluences with South Creek and North Creek, and the main stem both upstream and downstream of the USGS gaging station at Empire. The model was applied in half-month increments for the entire span of the data record for each reach (September – October, 2006; June – October, 2007; June – September, 2008). Complete results are shown in Tables 6.1 to 6.6.

- Estimated groundwater inflow rate showed considerable spatial and temporal variability, both seasonally and between years.
- North Creek, which is relatively un-shaded and suspected to be a significant gaining reach, showed relatively high values of estimated groundwater inflow

(0.96 cfs/mile on average, or 52% of observed streamflow), with some variability present (0.45 to 1.30 cfs/mile, with a standard deviation of 0.32 cfs/mile). The largest predicted groundwater inflows appeared to be lagged by 2 to 4 weeks behind periods of heavy rainfall, suggesting the presence of shallow groundwater in the system.

- Lower South Creek, which lacked downstream temperature data for 2007 and 2008, could only be analyzed for 2006, and the model predicted a negligible inflow of groundwater for the entire season. This is contrary to the results of the EOR study (2007) that identified it as a gaining reach, and is likely the result of errors in the input data for 2006. However, a significant inflow of cold water from the upper reaches of South Creek, rather than groundwater, could be responsible for maintaining low stream temperatures in lower South Creek.
- The upper Vermillion River main stem showed the greatest variability in estimated groundwater inflow rate (0.14 cfs/mile to 3.87 cfs/mile for the whole record), with a standard deviation of 0.98 cfs/mile and a mean flow of 1.05 cfs/mile. As this reach has been identified as a 'gaining' reach, the large variability in groundwater inflow rate does not seem likely. However, these rates never represented more than 50% of the observed stream flow in the reach. The temperature regime of this heavily-shaded reach is likely dominated by groundwater inflow, which might explain some of the variability seen in the estimated groundwater inflow rates: any errors in the input data (especially stream temperature) would have to be compensated for by large changes in calculated groundwater inflow rate. Indeed, the discrepancy in results from 2006 to 2007 was found to result from a reversal of the upstream-downstream temperature difference between years, likely the result of inconsistent installation of temperature probes.
- Consecutive reaches in the middle main stem of the Vermillion River were modeled: the reach upstream of the USGS gaging station for 2007 and 2008, and the downstream reach for 2007 only. The results were unrealistically large for both reaches, but suggest a highly variable groundwater inflow in the first reach (0.33 to 8.0 cfs/mile in 2007 and 2.3 to 6.2 cfs/mile in 2008) and larger, more consistent inflow for the second reach (5.1 to 11.1 cfs/mile, or 20% to 42% of stream flow, in 2007). For both reaches, higher rates occurred during periods of significant rainfall, suggesting the presence of significant surface water (tributary) inflow, which is lumped with the groundwater inflow by the model. The upstream reach had a much more consistent modeled groundwater inflow rate in 2008, which was a very dry year in which baseflow conditions were present for much of the summer and fall. Thus tributary inflow for much of this period is likely negligible.
- For the lower South Branch, the results are characteristic of a groundwater-fed stream: groundwater input is relatively constant throughout the 2007 modeling period (0.60 to 1.50 cfs/mile in 2007) and makes up a significant percentage of stream flow (25% to 63% in 2007), especially during dry periods. During periods of heavy rainfall groundwater input increases only slightly, suggesting that the groundwater input to South Branch is perhaps a combination of both shallow and deep groundwater. The 2008 results must be considered separately because of a

change in the way in which stream flow was measured at the gaging site between years, and because the groundwater temperatures used for the model are much higher in 2008 than in 2007. The 2008 results show more variability (0.2 to 1.6 cfs/mile) but are strongly tied to stream flow and precipitation, suggesting the presence of significant surface inflows. These surface inflows might be contributed by drainage tiles or irrigation from the significant amount of agricultural land in the drainage area.

A comparison was made of the spatial distribution of estimated groundwater inflow rates in the watershed for two periods in 2007, one corresponding to dry (baseflow) conditions and another to high-flow conditions (Figure 6.2). This comparison illustrated the considerable spatial variability of groundwater inflow in the system as well as the tendency of rainfall to increase predicted inflow rates at all modeled sites. In general, the largest inflows are located in the middle and upper main stem reaches of the Vermillion River. The largest increases in estimated groundwater inflow rates from the low- to high-flow scenarios were seen in the middle main stem, North Creek, and South Branch – all of which have considerable tributary inflow, which is lumped into groundwater inflow by the model and tends to inflate the estimated groundwater inflow rate. The results also suggested that shallow groundwater is likely present in South Branch and the middle main stem of the Vermillion River.

8.2. Sensitivity Analysis

A number of single flow measurements taken in the watershed at points near modeled reaches during September 2007 allowed for a limited assessment of the accuracy of the predicted groundwater inflow rates for these reaches. The assumption was made that the groundwater inflow rates held true outside of the modeled reaches to the locations where the point measurements were made; in this way a flow rate could be estimated for these locations. Results are shown in Table 6.11, and the locations for the measurements are in Figure 6.3. In general, performance was surprisingly good: errors of 16% and 3% were observed for two points in South Branch, 15% for a location on the middle main stem, and 25% for the downstream end of the upper main stem reach.

Application of the model to the Vermillion River system was challenging because of the presence of storm water and tributary inflows, mixed land use, and a complex hydrogeology. The temporal and spatial variability in the simulated groundwater inflows reflects these facts. However, this variability due to the hydrological diversity of the Vermillion River system was likely accentuated by poor quality or low resolution of the model input data. The sensitivity analysis illustrated these limitations and led to criteria for the applicability of the model based on its limitations.

The most important limitation of the model is related to stream flow: estimated groundwater inflow rates increase with stream flow, and unrealistically high groundwater inflows (i.e. greater than 2.0 cfs/mile) are estimated for stream flows exceeding approximately 20 cfs. This dependence occurs because as stream flows increase the heat budget residual of a stream reach becomes larger due to the greater energy content of the

stream flow, thus erroneously inflating the groundwater inflow rate; in reality the groundwater inflow comprises a smaller portion of a stream reach's heat budget when stream flows are large. This model limitation explains the unnaturally high (up to 11.1 cfs/mile) groundwater inflow estimates for Reaches 4 and 5 of the Vermillion River main stem, which have year-round stream flows significantly higher than 20 cfs.

Surface water inflows from storm sewers and ditches are not explicitly accounted for in the current model; this omission tends to increase groundwater inflow estimates. It is important that the model be applied to reaches with no persistent tributary inflows.

Estimated groundwater inflow rates decreased when wet periods were omitted, but rarely by more than 16% of seasonal averages. For seasonal groundwater inflow estimates, omission of wet periods may therefore not be necessary, but for shorter time periods model results will be more realistic for dry periods.

The difference between stream temperature and groundwater temperature is a logical constraint of the method given that the groundwater inflow needs to have an impact on the stream temperature regime in order to be detectable in a heat budget. Decreasing trends for groundwater inflow rates were detected in all modeled stream reaches when the water temperature difference between the stream and the groundwater was increased. In reaches with low stream flow, groundwater inflow rates in excess of 2.0 cfs/mile were predicted when the stream temperature-groundwater temperature difference was less than 2.0 to 3.0 ˚C. These relationships emphasize the need for a significant temperature difference between the stream and incoming groundwater, and stress the importance of accurate stream temperature and groundwater temperature measurements to drive the model, because errors in either will directly impact the groundwater inflow rate estimate.

The sensitivity analysis also revealed that model simulation results are highly dependent on the groundwater temperature and the shading/sheltering coefficient. An increase in groundwater temperature resulted in an increase in groundwater inflow rate, but this effect was small for low shading/sheltering and large for high shading. The accurate determination of groundwater temperature is therefore of greater importance in well-shaded stream reaches than in poorly-shaded ones. The former is more likely encountered for coldwater streams.

Finally, the correlation of estimated groundwater inflow rates to stream stage and antecedent precipitation was investigated using multiple linear regression. A relationship would be expected since groundwater inflow to a stream is typically driven by a difference in water level between the water table and the stream, with water moving down this gradient at a speed proportional to the transmissivity of the aquifer. As water table elevation data was not available, precipitation was used instead since water level will tend to fluctuate with the input of infiltrated rainfall. Antecedent rainfall was summed into bins of increasing size (0.5 months to 2 months by ½-month intervals), and the analysis was performed on reaches for which results were available for 2007 and 2008 (see Table 6.10). Two reaches on the Vermillion River (upper and middle main stem) were found to have the highest R^2 values for a bin size of 1.5 months or greater,

meaning that the time of concentration for shallow groundwater in the main stem is on the order of 5 to 8 weeks. No correlation was found in North Creek due to the high impervious surface area of its drainage area (and therefore low amounts of infiltration relative to surface runoff). South Branch had high R^2 values for all bin sizes of antecedent precipitation (0.61-0.75) making any definite conclusions difficult, but the presence of an extensive tile drainage network and potentially large tributary inflows complicate the analysis and likely provide a substantial baseline flow to the reach.

A number of difficulties were encountered in the application of the model. Only a small portion of the watershed was modeled due to the lack of favorable reaches with adequate input data and relatively few tributaries. This was primarily the result of a monitoring strategy that was largely incompatible with the data needs of the model. Placement of additional stream temperature stations along the main stem of the Vermillion River, primarily above major confluences, would help alleviate this issue. Errors in the data itself were also encountered, especially in the groundwater temperature and stream temperature data. These were likely the result of inconsistencies in installation between years, improper installation of temperature probes, and a phenomenon in which water began mixing vertically within the piezometer tubes on a diurnal basis during fall. Accuracy of input data must be considered in the analysis of any simulation results.

In light of these difficulties and the results of the sensitivity analysis, criteria were developed to guide future applications of the model:

(1) The model is applicable to stream reaches that receive significant groundwater inflow relative to stream flow.
(2) The stream temperature – groundwater temperature difference needs to be sufficiently large for use of the heat budget approach. A difference greater than 2.0 to 3.0 ˚C appears to produce the most realistic results.
(3) The model should be applied to small stream reaches and tributaries and preferably, when and where stream flow does not exceed roughly 15 - 20 cfs.
(4) Stream reaches should have no persistent surface water inflows.
(5) Dry weather or baseflow conditions will produce the best results. For short-term analyses (i.e. less than a season), periods should be selected when inflows from storm sewers and drainage ditches are non-existent or minimal.
(6) Great care should be taken in estimation or measurement of the groundwater temperature, particularly for well-shaded reaches.

In conclusion, it is noted that the extent of the modeling results thus far is fairly limited, due to constraints imposed by the input data. While most of the results should probably be viewed with considerable reservations, what has been presented here should provide an idea of where groundwater input is significant (such as in North Creek and the middle Vermillion River) and demonstrate that while the model's heat budget approach is fundamentally sound, the above limitations to the method must be borne in mind. The importance of data quality and a monitoring strategy that takes into account the application of the collected data should also be stressed. It is expected that in the future the model can be applied to other reaches in the watershed.

Acknowledgements

This study was conducted with support from the Vermillion River Watershed Joint Powers Board (VRWJPB) and the Minnesota Pollution Control Agency (MPCA). Bruce Wilson is the MPCA project officer. Data were provided by Kim Chapman of Applied Ecological Services, Inc. Additional data provided by the Minnesota Department of Natural Resources, Dakota County Soil and Water Conservation District, Scott County Soil and Water Conservation District, and the Metropolitan Council. Work was also funded in part by the United States Environmental Protection Agency (EPA) under the Science to Achieve Results (STAR) Graduate Fellowship Program. EPA has not officially endorsed this publication and the views expressed herein may not reflect the views of the EPA.

References

Anderson, M.P. (2005). Heat as a Ground Water Tracer. Ground Water 43(6): 951 – 968.

Bartolino, J.R. and Niswonger, R.G. (1999). Numerical Simulation of Vertical Ground-water Flux of the Rio Grande From Ground-water Temperature Profiles, Central New Mexico. Water Resources Investigation Report 99-4212. USGS, Albuquerque, New Mexico.

Bowen, I.S. (1926). The Ratio of Heat Losses by Conduction and by Evaporation From Any Water Surface. Phys. Rev. 27, 779-787.

Conant, B. (2004). Delineating and Quantifying Ground Water Discharge Zones Using Streambed Temperatures. Ground Water 42: 243 - 257.

Constantz, J. (2008). Heat as a Tracer to Determine Streambed Water Exchanges. J. Water Resour. Res. 44: 20 pp.

Dakota County. (2006). Dakota County ambient groundwater quality study: 1999 – 2003 Report. Dakota County, MN, USA, 108 pp. Available online: http://www.co.dakota.mn.us/CountyGovernment/Reports/Environment/Ambient.htm.

Duffie, J.A. and Beckman, W.A. (1991). Solar Engineering of Thermal Processes (2nd ed.). John Wiley and Sons, New York, NY.

Dumouchelle, D.H. (2001). Evaluation of Ground-water/Surface-water Relations, Chapman Creek, West-Central Ohio, by Means of Multiple Methods. Water Resources Investigation Report 01-4202. USGS, Columbus, Ohio.

Duque, C., Calvache, M.L., and Engesgaard, P. (2010). Investigating River-aquifer relations using water temperature in an anthropized environment (Motil-Salobrena aquifer). J. Hydrology 381: 121 – 133.

Edinger, J.E., Duttweiler, D.W., and Geyer, J.C. (1968). The Response of Water Temperatures to Meteorological Conditions. J. Water Resour. Res. 4, 1137-1143.

Edinger, J.E., Brady, D.K. and Geyer. J.C. (1974). Heat Exchange in the Environment. Report No. 14, Cooling Water Discharge Research Project RP-49, Electric Power Research Institute, Palo Alto, CA, 125 pp.

Emmons and Olivier Resources, Inc. (2007). Vermillion River Headwaters Groundwater Recharge Area Inventory and Protection Plan. Final Report. EOR, Inc. Sep 14, 2007. Oakdale, MN, 89 pp.

Erickson, T.O. and Stefan, H.G. (2008). Baseflow analysis of the Upper Vermillion River, Dakota County, Minnesota. Project Report 507. St. Anthony Falls Laboratory, University of Minnesota: Minneapolis, MN, USA, 55 pp. Available online: home.safl.umn.edu/bmackay/pub/pr/pr507.pdf.

Erickson, T.O. and Stefan, H.G. (2009). Groundwater recharge in a coldwater stream watershed during urbanization. Project Report 524. St. Anthony Falls Laboratory, University of Minnesota: Minneapolis, MN, USA, 74 pp. Available online: home.safl.umn.edu/bmackay/pub/pr/PR524.pdf.

Essaid, H., Zamora, C.M., McCarthy, K.A., Vogel, J.R., and Wilson, J.R. (2008). Using Heat to Characterize Streambed Water Flux Availability in Four Stream Reaches. J. Environ. Qual. 36: 1010 – 1023.

Galli, J. (1990). Thermal Impacts Associated With Urbanization and Stormwater Best Management Practices. Metropolitan Washington Council of Governments, Washington, D.C., 188 pp.

Herb, W.R. (2008). Analysis of the effect of stormwater runoff volume regulations on thermal loading to the Vermillion River. Project Report 520. St. Anthony Falls Laboratory, University of Minnesota: Minneapolis, MN, USA, 34 pp. Available online: home.safl.umn.edu/bmackay/pub/pr/pr517.pdf.

Herb, W.R. and Stefan, H.G. (2008a). A flow and temperature model for the Vermillion River, Part I: Model development and baseflow conditions. Project Report 517. St. Anthony Falls Laboratory, University of Minnesota: Minneapolis, MN, USA, 30 pp. Available online: home.safl.umn.edu/bmackay/pub/pr/pr517.pdf.

Herb, W.R. and Stefan, H.G. (2008b). A flow and temperature model for the Vermillion River, Part II: A response to surface runoff inputs. Project Report 525. St. Anthony Falls Laboratory, University of Minnesota: Minneapolis, MN, USA, 61 pp. Available online: home.safl.umn.edu/bmackay/pub/pr/pr525.pdf.

Idso, S.B. (1981). A Set of Equations for Full Spectrum and 8- to 14-mm and 10.5- to 12.5-mm Thermal Radiation From Cloudless Skies. Water Resour. Res. 17, 295-304.

Klein, R.D. (1979). Urbanization and Stream Quality Impairment. Water Resour. Bull. 15: 948-963.

Palen, B.M. (1990a). Geological Atlas of Dakota County, Minnesota: Quaternary Hydrogeology. Minnesota Geological Survey, University of Minnesota. St. Paul, MN. County Atlas Series, Atlas C-6, Plate 5 of 9.

Palen, B.M. (1990b). Geological Atlas of Dakota County, Minnesota: Bedrock Hydrogeology. Minnesota Geological Survey, University of Minnesota. St. Paul, MN. County Atlas Series, Atlas C-6, Plate 6 of 9.

Paul, M.J. and Meyer, J.L. (2001). Streams in the Urban Landscape. Ann. Rev. Ecol. Syst. 32, 333-365.

Pirazzini, R., Nardino, M., Orsini, A., Georgiadis, T. and Levizzani, V. (2000). Parameterisation of the Downward Longwave Radiation from Clear and Cloudy Sky at Ny-Alesund (Svalbard). Proceedings of the International Radiation Symposium, St. Petersburg, Russia, 5 pp.

Rasmussen, A.H., Hondzo, M., and Stefan, H.G. (1995). A Test of Several Evaporation Equations for Water Temperature Simulations in Lakes. Water Resour. Bull. 31, 1023-1028.

Stefan, H.G., Gulliver, J., Hahn, M.G., and Fu, A.Y. (1980). Water Temperature Dynamics in Experimental Field Channels: Analysis and Modeling. Proj. Rep. 193. St. Anthony Falls Lab., University of Minnesota, Minneapolis, MN, 217 pp.

Stonestrom, D.A. and Constantz, J. (2003). Heat as a tool for studying the movement of ground water near streams. USGS Circular 1260. USGS.

Taylor, C. and Stefan, H.G. (2009). Heating of shallow groundwater flow by conduction from a paved surface: Requirements for coldwater stream protection. Project Report 531. St. Anthony Falls Laboratory, University of Minnesota: Minneapolis, MN, USA, 35 pp. Available online: www.safl.umn.edu/publications/PR531.pdf.

Su, G.W., Jasperse, J., Seymour, D. and Constantz, J. (2004). Estimation of Hydraulic Conductivity in an Alluvial System Using Temperature. Ground Water 42: 890–901.

Appendix A. Summary of Assembled Data

This section includes an overview of relevant data collected in the watershed by various groups, including state and local agencies, watershed organizations, and consultants. This information is current as of November 10, 2009.

A.1. Stage/flow Data

The USGS has maintained a stream gaging station on the Vermillion River near the city of Empire for over 20 years. The stream flow measured at the USGS station includes the discharge from the Empire WWTP operated by the Met Council.

Stage has been measured at 7 stations in the watershed since 2000 by Dakota County SWCD and Minnesota DNR (Figure A-1.) Note that a couple of the sites are dry most of the year or are not regularly maintained (e.g. VR12, VR24). Rating curves have been updated a number of times over the monitoring period, and most recently in summer of 2007. Mean daily flows are available for non-winter months (roughly March – November) over the 9-year record (2000-2008). Gaps exist in some of the data sets in cases where the streams were dry or pressure transducers had to be replaced. A new station was installed in June 2007 on South Creek, so only a short record (and a correspondingly rough rating curve) is available for this particular site, and the data was not used in this study. Between 2007 and 2008, the datum for stream stage at the South Branch site was changed, and a completely new rating curve was developed starting in 2008. Therefore flow data for 2008 will be rough, and results should be considered accordingly.

A.2. Surface (Stream) Water Temperature

Stream temperature monitoring in the Vermillion River watershed intensified in the last several years. In addition to a few existing sites, temperature sensors/recorders were installed at approximately 30 stations in the Vermillion River and its major tributaries as early as June 2006, and have been maintained by Dakota County SWCD, Minnesota DNR, and Applied Ecological Services, Inc. (AES). Most of these sites are shown in Figure A-2. A number of temperature loggers in the upper Vermillion River and in some smaller tributaries are removed prior to the winter period, usually in November, then re-deployed the following May. Currently data is available from the 2006 through 2008 monitoring periods.

A.3. Groundwater Temperature

In September 2006, piezometer tubes with temperature recorders inside were added to most of the existing surface water monitoring stations to record temperatures in the stream sediments (Figure A-2). These installations have been maintained by AES and Emmons and Olivier Resources, Inc. (EOR). The temperature records have been labeled

"groundwater temperatures", regardless of whether pore water is flowing into or out of the streambed.

As in the case of the stream temperature probes, roughly a dozen loggers are removed in late November to prevent freezing during the winter. These loggers are usually re-launched the following May. It has been noted that many of these loggers were not installed in the screened portion of the piezometers when re-launched in May 2007. This may render the June-October 2007 data from these particular sites unusable, as the probes would be providing the temperature of water that is heavily influenced by surface water and atmospheric heat exchange, rather than the temperature of groundwater as it flows through the perforations.

Prior to this larger monitoring effort, piezometer tubes were installed at a number of sites in South Creek and the upper Vermillion River in 2005 to measure streambed temperature. More specifically, equipment was installed at the following locations: (1) on South Creek where Cedar Avenue crosses the river in Lakeville, (2) on the Vermillion River main stem in Farmington at the Chippendale Avenue crossing, and (3) on the lower Vermillion River at the Hamburg Avenue crossing. These sites were installed in August 2005 and removed in June 2006, so the data were not useful for application of our model.

The Minnesota Pollution Control Agency (MPCA) maintains two shallow wells in which groundwater temperature has been measured year-round since January 2006. These wells are both located near the city of Farmington (see Figure A-2), and measure water at a depth of about 10 feet below the surface. Two deeper wells are also maintained at these same two sites, measuring water temperature at a depth of approximately 50 feet. These deep well data were not used in the analysis.

The MCPA maintains a number of additional wells near Farmington, including a shallow (15 foot) and deep (30 foot) well located in a residential area, and a shallow (15 foot) and deep (50 foot) well located in a commercial area. These two nested wells were installed in April 2007, and a groundwater temperature record exists through fall 2008, except that the instrumentation at the shallow residential well failed in 2007. These data were also not used in the groundwater temperature analysis.

Groundwater temperature data is analyzed in more detail in Appendix B.

A.4. Climate Data

Daily precipitation, daily maximum air temperature, and daily minimum air temperature have been recorded at a National Weather Service site at the Rosemount Agricultural Station located on the northern end of the watershed. This data is available year-round, beginning January 1, 2006. Data from the Rosemount station itself, which is maintained by the University of Minnesota, includes hourly solar radiation, air temperature, relative humidity, dew point temperature and precipitation, but data has only been released for 2005 and 2006. Hourly air temperature, dew point temperature, and wind speed data has been acquired from the Air-Lake Airport in Lakeville, MN for 2006 and 2007 in order to

fill in gaps in the Rosemount data, and to provide input data for 2007. Solar radiation data for 2007 and 2008 had to be taken from St. Anthony Falls Laboratory at the University of Minnesota in Minneapolis, MN, located approximately 15-20 miles from the Vermillion River. At the beginning of 2008, a weather station was installed in the watershed near Farmington, providing 15-minute air temperature, relative humidity, wind speed, and precipitation. This data was used to run the 2008 simulations.

A.5. Stream Geometry

Stream reach length has been estimated from aerial photography, and mean bed slope has been estimated from contour maps. Cross-sectional geometry of the reaches is approximated from stream surveys when available, though primarily from detailed flow measurements at the gaging sites in which depth is recorded at fine spatial resolution across the channel. Stream width can then be determined from knowledge of the stream flow rate and geometry.

Appendix B. Groundwater Temperature Data Analysis

An important input parameter for the model is the temperature of groundwater entering the stream. Monitoring efforts in the watershed have produced two major sets of data for groundwater temperature: (1) Minnesota Pollution Control Agency (MPCA)-maintained wells located near the Vermillion River in Farmington, MN, and (2) piezometers installed in the streambed at the same locations where stream temperatures were being measured (maintained by AES). Much of the MPCA well data was taken at a depth of 15 feet or more, so only the 'shallow' well data (taken at a 10-foot depth) was used along with the piezometer data to produce an estimate of groundwater temperature as a function of time of year for running the model for 2006 and 2007. In 2008, the piezometer installations were improved to remove some of the issues encountered in the 2007 data, and therefore the 2008 data was used as a direct input to the model.

B.1. Water Temperatures in Shallow Wells

Given that the MPCA wells were not located in the streambed and were measuring groundwater at a depth of 10 feet, this data might be expected to slightly under-estimate groundwater temperature. However, the data set proved useful for understanding seasonal trends in groundwater temperature and for providing a lower bound for the estimate of groundwater temperature. As to be expected, groundwater temperature did not vary much on an hourly or daily time scale, but showed weekly variation and a seasonal (roughly sinusoidal) pattern over the course of the year (Figure B-1). Groundwater temperature is considered a constant in the model, and the data supports this assumption provided that the model is run for simulation periods of no more than a couple weeks at a time. A half-month simulation period was therefore chosen for application of the model, and groundwater data was averaged over this time interval (Table B-1). It should be noted that due to an installation error, a portion of the late-summer measurements in the north well in 2007 will be unreliable, and are not factored into the calculation of mean values.

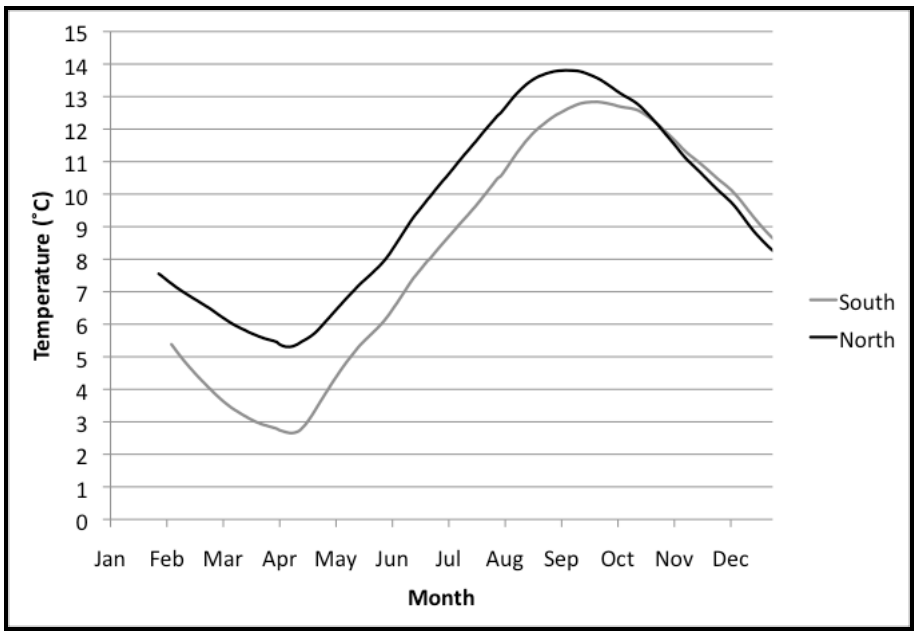

Figure B-1. Time series of groundwater temperature measured at a 10-foot depth in two MPCA-maintained wells (designated 'North' and 'South') in 2006. The wells are located near Farmington, MN.

Table B-1. Half-month averages of groundwater temperature measured in two MPCA-maintained wells in 2006 and 2007. Values are shown only for periods in which the model was applied (June - October). Well depth is approximately 10 feet.

Period	2006 North °C	2006 South °C	2006 Mean °C	2007 North °C	2007 South °C	2007 Mean °C
June 1 - 15	8.6	6.7	**7.7**	9.3	8.3	**8.8**
June 16 - 30	9.8	7.9	**8.9**	10.2	9.1	**9.7**
July 1 - 15	10.8	8.9	**9.9**	n/a	10	**10.0**
July 16 - 31	11.8	9.9	**10.9**	n/a	10.9	**10.9**
Aug 1 - 15	12.8	11	**11.9**	n/a	11.8	**11.8**
Aug 16 - 31	13.6	12	**12.8**	n/a	12.6	**12.6**
Sep 1 - 15	13.8	12.6	**13.2**	14.2	13.3	**13.8**
Sep 16 - 30	13.6	12.8	**13.2**	14.1	13.7	**13.9**
Oct 1 - 15	13.1	12.7	**12.9**	13.7	13.7	**13.7**
Oct 16 - 31	12.4	12.3	**12.4**	13.3	13.7	**13.5**

According to Table B-1 the groundwater temperatures are remarkably consistent between the two wells and even between years. The highest shallow groundwater temperatures occur in September suggesting that groundwater temperature lags significantly behind climate conditions (air temperature), and slightly behind stream temperature, which experiences a maximum temperature in mid- to late-August (not shown). With the exception of a short period this data set was deemed acceptable to use in estimation of groundwater temperature for the model.

B.2. Water Temperatures in Stream Sediments (Piezometer Data)

The recording of water temperatures in the streambed of the Vermillion River and its tributaries at a relatively large number of points was intended to generate a dataset that would characterize groundwater inflow, which can be difficult to do accurately. The intention was also to help identify "gaining reaches" vs. "losing reaches" based on comparison of stream water temperatures with piezometer temperatures measured in the same locations. A schematic of a typical installation is shown in Figure B-2. A length of one-half inch diameter electrical conduit was driven roughly one to two feet into the streambed. This tube was sealed at the bottom end with a bolt and electrical tape, and slits were cut into the lower section to allow groundwater to flow into the tube. An integrated temperature probe and logger was placed in the bottom of the tube to record water temperature.

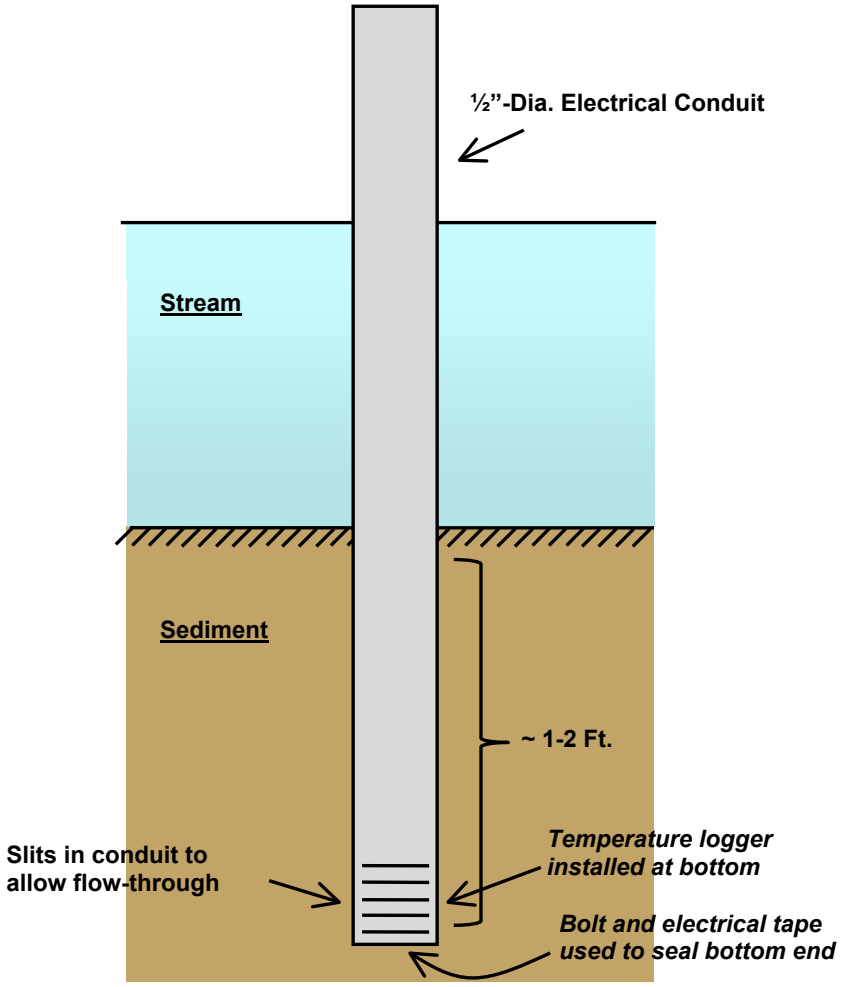

Figure B-2. Schematic of piezometer tube used to measure streambed (groundwater) temperature in the Vermillion River and its tributaries. In 2008 this setup was improved by adding a baffle above the slotted portion of the tube to prevent water from mixing vertically within the tube during early fall.

Unfortunately, a number of discrepancies show up in the piezometer data that make some of the measurements suspect, and impossible to use as a source of groundwater temperature information. General issues include not knowing the precise depth at which groundwater temperature was being measured, and concerns that piezometers were installed too close to the surface and/or were taking on surface water or were being heated by solar radiation penetrating from the water surface.

One suspect behavior often found in the piezometer temperature data is a reversal of groundwater temperature and stream temperature; groundwater temperature is suddenly higher than stream temperature, and shows a daily amplitude. This usually occurs in September or October when air temperatures become colder. For illustration, consider the temperature record for Fall 2006 at AES-66 in North Creek (Figure B-3); this data set is typical of many of the groundwater temperature records. In September the groundwater temperature is relatively constant around 9 ˚C and shows little (if any) diurnal variation, with the exception of a few days in which stream temperature dipped to near groundwater temperature, either because of weather conditions or a rainfall event. On October 11, the temperatures abruptly reverse and groundwater temperature begins to show a diurnal variation on the order of 1˚C, which is significantly larger than any variation in the record prior to that date. The rapid drop in stream temperature is not surprising, given the cold weather and relatively low volume of water in the stream; the rapid drop in groundwater temperature (about 2˚C in 24 hours) is suspicious. The likely cause of this behavior is vertical mixing in the piezometer tube. During summer the water in the tube stays stratified, with warmer water at the top and colder groundwater at the bottom, where the temperature probe is located. At the reversal point in the fall, water at the top of the tube is being cooled by conduction to the now-colder stream water adjacent to the tube, to a temperature below the groundwater temperature. This colder water sinks to the bottom of the piezometer tube where the probe is located, and causes a lower temperature to be recorded. This process repeats on a daily basis as atmospheric heat exchange warms the water column and causes stratification, with groundwater once again as the coldest water in the tube (thus leading to a short-term accurate measurement); the mixing process occurs once more after sunset. This behavior is apparent in many of the piezometer temperature records during fall (for both 2006 and 2007), and makes it difficult to extract a ‘true’ groundwater temperature from the data. It should be noted that mixing in the piezometer tube can occur earlier in the year where the groundwater temperature is higher than the stream temperature. In 2008 a baffle was placed above the temperature loggers to prevent water from mixing in the piezometer tubes, and data quality appears to have improved at most of the sites.

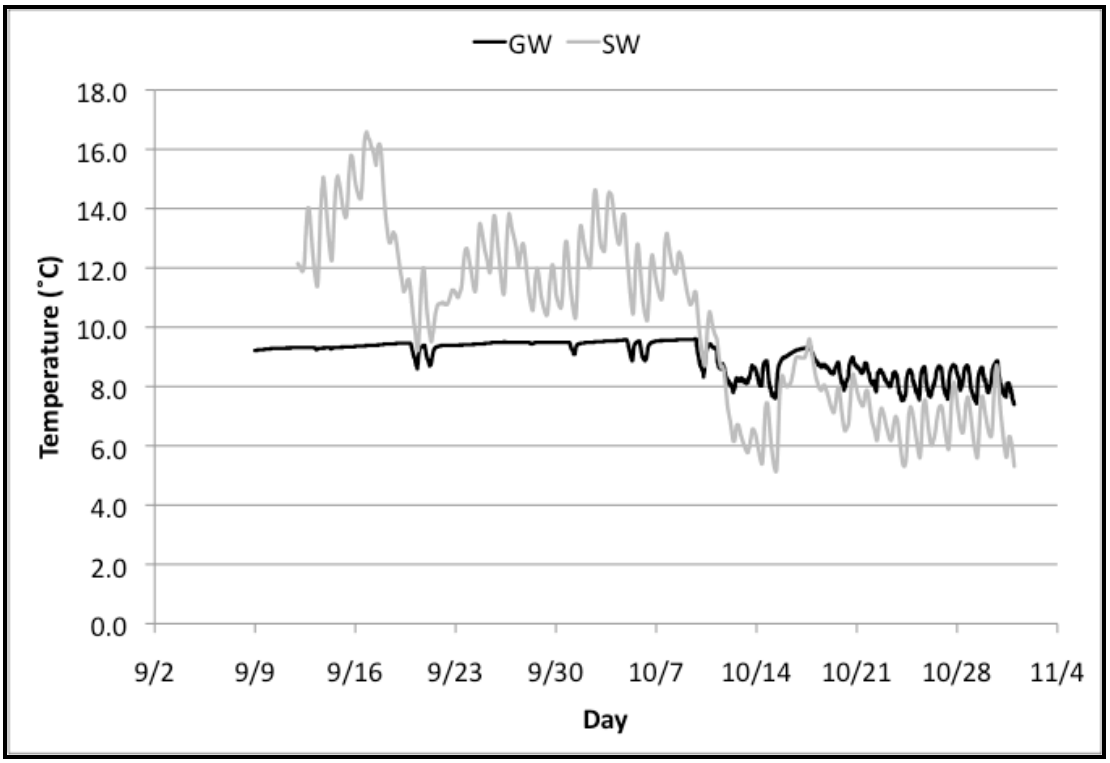

Figure B-3. Measured groundwater and stream temperatures at AES-66 (North Creek) during 2006. Note the abrupt change in groundwater temperature ('GW') and stream temperature ('SW') around October 11, which indicates that vertical mixing is occurring in the piezometer tube.

Another common trend seen in the data is one in which very little difference exists between the groundwater and stream temperatures records, with both experiencing significant daily fluctuations. It was not uncommon at times to see a measured groundwater temperature significantly larger than stream temperature. A good example is the 2007 summer record at AES-79 on the main stem (Figure B-4). This behavior is likely the result of an improper installation of the temperature probe (i.e. too high in the piezometer tube), or perhaps is an indication that the station is located in a losing or neutral reach. In the case of AES-79, which is located in a portion of the main stem identified as a 'gaining' reach (EOR, 2007), the former case is more likely; the temperature probe is too close to the surface and/or has not been installed in the perforated portion of the piezometer tube and is thus measuring surface water or shallow sediment temperature rather than groundwater temperature. A similar effect is present in other records (e.g. AES-56 and AES-58 in 2007) in which the groundwater temperature experiences greater daily fluctuations than the stream temperature (not shown).

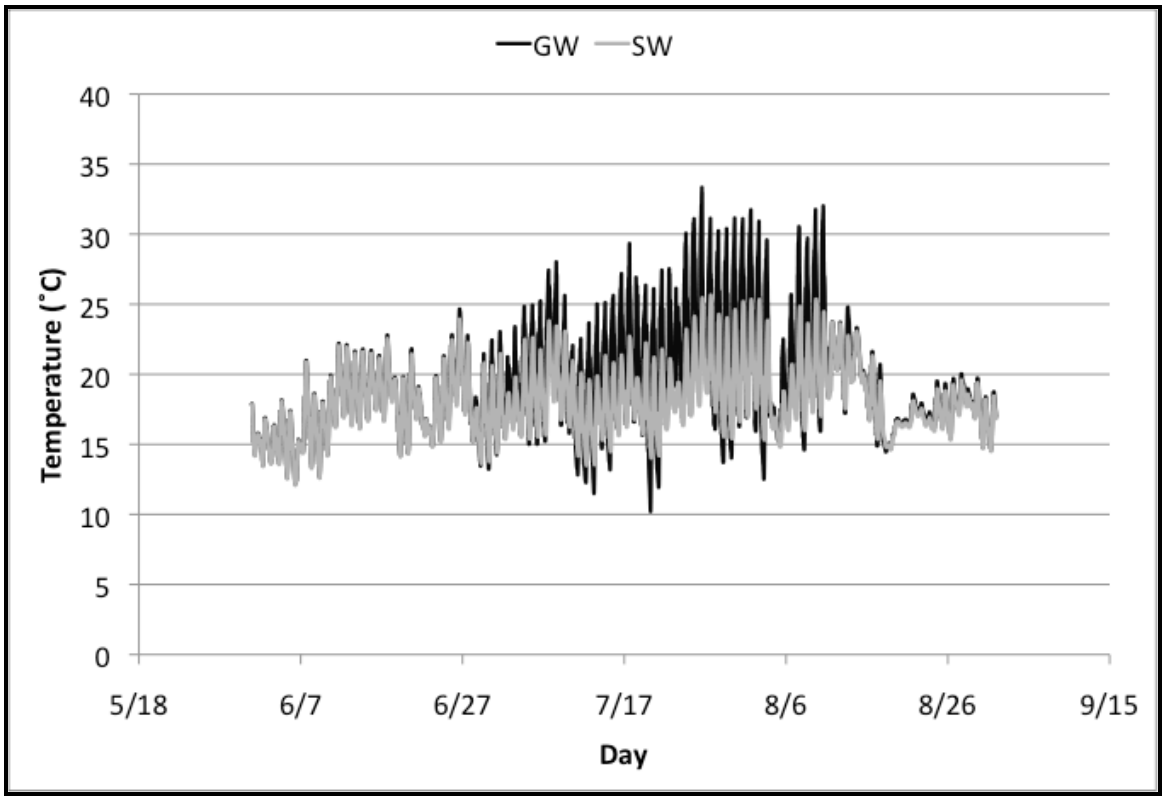

Figure B-4. Measured groundwater and stream temperatures at AES-79 (North Creek) during summer 2007. Note the abnormally high values and diurnal fluctuations of groundwater temperature ('GW') that are larger than those seen in the stream temperature record ('SW'), which indicates an improper installation of the GW temperature probe.

One final caveat is that piezometer tubes were often placed in the coldest part of the stream (i.e. where groundwater was likely coming in), and if the groundwater input to a stream reach is localized rather than distributed along the reach, the temperature measurement in the piezometer tube may provide an artificially low estimate of the characteristic groundwater temperature for the reach.

Overall it should be noted that the temperature measured inside a piezometer tube will be a true groundwater temperature only if there is a significant groundwater inflow to the stream that sweeps past the temperature sensor at all times. If the groundwater flow is weak or absent, the temperature in the piezometer tube will be influenced by the stream water temperature, via conduction though the sediment/pore water and sidewalls of the piezometer tube. In addition, two potential sources of error in the available groundwater temperature data sets are vertical mixing inside the tube, and installation too close to the surface; either will render portions of the available record unusable.

In the remainder of this appendix results and issues that are specific to the six reaches modeled in this project (North Creek, South Creek, upper main stem of the Vermillion River, two reaches in the middle main stem of the Vermillion River, and South Branch) are given.

B.2.1. North Creek

In general, the quality of data for the two North Creek monitoring stations (AES-65 and AES-66) is fair for 2006 and poor for 2007, with vertical mixing in the piezometer tubes present in all records. In 2007, vertical mixing in the piezometer tubes is apparent in the records of both stations during the second week of September, meaning that groundwater temperatures cannot be trusted beyond this point in the record. Furthermore, recorded groundwater temperatures seem considerably higher in the 2007 records than in 2006, with some unusually high spikes (one exceeding 20 ˚C at AES-66), suggesting that the probes might have been installed too high in the tubes. In 2006, AES-65 appears to experience piezometer tube mixing for the entire length of the record, while AES-66 remains relatively constant until early October. A summary of streambed (groundwater) temperature averages, not taking into account these caveats, is shown in Table B-2.

Table B-2. Half-month averages of groundwater temperature measured at AES-65 and AES-66 in North Creek in 2006 and 2007. Values are for all data in the record, regardless of quality concerns. Fall data in particular should be potentially disregarded due to the presence of vertical mixing in the piezometer tubes.

Period	2006 Stn 65 (˚C)	2006 Stn 66 (˚C)	2006 Mean (˚C)	2007 Stn 65 (˚C)	2007 Stn 66 (˚C)	2007 Mean (˚C)
June 1 - 15	--	--	**--**	11.3	10.9	**11.1**
June 16 - 30	--	--	**--**	12.2	11.5	**11.9**
July 1 - 15	--	--	**--**	12.8	12	**12.4**
July 16 - 31	--	--	**--**	14	13	**13.5**
Aug 1 - 15	--	--	**--**	15.4	15.4	**15.4**
Aug 16 - 31	--	--	**--**	16.1	19.5	**17.8**
Sep 1 - 15	13.4	9.3	**11.4**	15.1	17.8	**16.5**
Sep 16 - 30	11.8	9.4	**10.6**	13.6	16.2	**14.9**
Oct 1 - 15	10.2	9.1	**9.7**	13.8	15.3	**14.6**
Oct 16 - 31	7.5	8.4	**8.0**	12.3	13.8	**13.1**

B.2.2. South Creek

A stretch of South Creek from AES-84 to AES-80 was modeled. While the data collected at AES-84 appears reasonable (with vertical mixing occurring in mid- to late-October in both years), the data at AES-80 are largely non-existent; no groundwater data were collected in 2006, and the record in 2007 does not begin until October. Unfortunately, data from other nearby stations (e.g. AES-79 or AES-94) is either missing or unusable. The MPCA wells, however, are located near AES-80, and are used to improve the estimate of groundwater temperature in South Creek. Groundwater temperature averages for AES-84 are shown in Table B-3.

Table B-3. Half-month averages of groundwater temperature measured at AES-84 in South Creek in 2006 and 2007. Values are for all data in the record, regardless of quality concerns. October data in particular should be potentially disregarded due to the presence of vertical mixing in the piezometer tubes.

Period	2006 (˚C)	2007 (˚C)	Mean (˚C)
June 1 - 15	--	8.7	**8.7**
June 16 - 30	--	9.2	**9.2**
July 1 - 15	--	9.7	**9.7**
July 16 - 31	--	10.1	**10.1**
Aug 1 - 15	--	10.7	**10.7**
Aug 16 - 31	--	10.9	**10.9**
Sep 1 - 15	--	10.7	**10.7**
Sep 16 - 30	10.4	10.7	**10.6**
Oct 1 - 15	10.1	10.9	**10.5**
Oct 16 - 31	9.6	10.5	**10.1**

B.2.3. Vermillion River main stem from AES-79 to CHP-1

A section of the upper Vermillion River main stem was also modeled, from AES-79 to CHP-1, a station located at the point where Chippendale Avenue crosses the river. Groundwater temperature was not measured at this station, but additional data was taken from AES-63, which is located roughly one-third mile north of CHP-1 on Middle Creek. For both 2006 and 2007, the data recorded at AES-63 appears to be of good quality, though it should be noted that groundwater temperature is often higher than stream temperature by as much as 3 ˚C, and exceeds the temperatures measured at the MPCA wells during the same interval by 3 ˚C or more (not shown). This trend is not necessarily troublesome, as Middle Creek is very shallow and will be impacted significantly by weather conditions. Half-month groundwater temperature averages for this data are shown in Table B-4. Temperatures recorded at AES-79 in 2006 shows no cause for concern except for tube mixing in early October, but the 2007 data are unusable because the probe appears to be measuring stream temperature rather than groundwater temperature. Because the MPCA wells are located along this reach, the well water temperatures will again be used to improve the estimate of groundwater temperature for modeling of this reach.

Table B-4. Half-month averages of groundwater temperature measured at AES-63 in Middle Creek in 2006 and 2007. Values are for all data in the record, regardless of quality concerns. October data in particular should be potentially disregarded due to the presence of vertical mixing in the piezometer tubes.

Period	2006 (˚C)	2007 (˚C)	Mean (˚C)
June 1 - 15	--	13.4	**13.4**
June 16 - 30	--	14.2	**14.2**
July 1 - 15	--	14.1	**14.1**
July 16 - 31	--	14.1	**14.1**
Aug 1 - 15	--	15.1	**15.1**
Aug 16 - 31	--	15.6	**15.6**
Sep 1 - 15	13.4	13.7	**13.6**
Sep 16 - 30	11.8	12.9	**12.4**
Oct 1 - 15	10.2	12.6	**11.4**
Oct 16 - 31	7.5	10	**8.8**

B.2.4. Vermillion River main stem from AES-58 to AES-49

Two consecutive sections of the Vermillion River main stem were modeled; the sections extended from AES-58 to AES-56, and from AES-56 to AES-49. Surface and streambed temperature records at these stations start at different times or are nonexistent for 2006, so half-month mean temperatures were calculated for 2007 only. Unfortunately, installations at AES-49, AES-56 and AES-58 appeared faulty, as groundwater and stream temperatures were nearly identical for the 2007 record. Similar trends were seen at stations in nearby tributaries, including at AES-54 and AES-57; the record at AES-59 (a tributary at the upstream end of the modeled reaches) appeared acceptable and was used to provide an estimate of groundwater temperature along with the MPCA shallow well data. Half-month groundwater temperature averages for AES-59 are shown in Table B-5.

Table B-5. Half-month averages of groundwater temperature measured at AES-59 in the middle main stem of the Vermillion River in 2007. Values are for all data in the record, regardless of quality concerns. September data in particular should be potentially disregarded due to the presence of vertical mixing in the piezometer tubes.

Date	2007 (˚C)
June 1 - 15	17.1
June 16 - 30	17.9
July 1 - 15	16.8
July 16 - 31	17.1
Aug 1 - 15	17.8
Aug 16 - 31	17.5
Sep 1 - 15	16.8
Sep 16 - 30	15.6
Oct 1 - 15	14
Oct 16 - 31	10.9

B.2.5. South Branch

The model was also applied to lower South Branch from AES-23 to AES-21, where the tributary enters the Vermillion River. The streambed temperature data in this reach also appeared to suffer from poor installations; the 2006 record at AES-23, and the 2007 records at both AES-21 and AES-23 appear to be measuring a mixture of groundwater and surface water temperature. Data from AES-109, a nearby station in the Vermillion River, is missing for most of 2007 due to loss of the data logger at that location. This left the 2006 record at AES-21 as the only reliable data (not shown). Simulations for fall 2006 used a combination of this data and the MPCA shallow well data, and the 2007 simulations used the same groundwater temperatures as were used for 2007 in the middle reaches of the Vermillion River main stem (see B.2.4).

B.3. Summary of Groundwater Temperature Information as Used in the Model

Using a combination of well and piezometer data, values of groundwater temperature were averaged over half-month intervals for the simulation period (generally fall 2006 and June - October 2007). In most cases the difference between these average groundwater temperatures and the well temperatures for a given period was assumed to represent roughly half of the potential range of groundwater temperature. Mean and likely ranges of groundwater temperature as a function of time are shown in Table B-6 for the modeled reaches.

Table B-6. Mean and likely range of groundwater temperature for modeled reaches as a function of time within the simulation period, as computed from well and piezometer data. A half-month time period was used for averaging.

North Creek (AES-66 to AES-65)

Period	2006 Mean (˚C)	2006 Range (˚C)	2007 Mean (˚C)	2007 Range (˚C)
June 1 - 15	--	--	10.0	8-12
June 16 - 30	--	--	10.0	9-13
July 1 - 15	--	--	11.0	9-13
July 16 - 31	--	--	12.0	10-14
Aug 1 - 15	--	--	13.0	11-15
Aug 16 - 31	--	--	14.0	12-16
Sep 1 - 15	12	9-14	15.0	12-16
Sep 16 - 30	12	9-14	14.0	12-16
Oct 1 - 15	11	8-13	13.0	12-15
Oct 16 - 31	10	8-13	--	--

South Creek (AES-84 to AES-80)

Period	2006 Mean (˚C)	2006 Range (˚C)	2007 Mean (˚C)	2007 Range (˚C)
June 1 - 15	--	--	9.0	8-10
June 16 - 30	--	--	9.0	8-11
July 1 - 15	--	--	10.0	8-11
July 16 - 31	--	--	10.0	9-12
Aug 1 - 15	--	--	11.0	10-13
Aug 16 - 31	--	--	12.0	10-14
Sep 1 - 15	--	--	12.0	10-15
Sep 16 - 30	12	9-14	12.0	10-15
Oct 1 - 15	11	9-14	12.0	10-15
Oct 16 - 31	10	8-13	12.0	9-14

VR Main Stem (AES-79 to CHP-1)

Period	2006 Mean (˚C)	2006 Range (˚C)	2007 Mean (˚C)	2007 Range (˚C)
June 1 - 15	--	--	10.0	8-13
June 16 - 30	--	--	11.0	9-14
July 1 - 15	--	--	12.0	10-14
July 16 - 31	--	--	13.0	10-15
Aug 1 - 15	--	--	13.0	11-16
Aug 16 - 31	--	--	14.0	11-16
Sep 1 - 15	13	12-15	14.0	12-16
Sep 16 - 30	12	11-14	13.0	11-15
Oct 1 - 15	11	9-13	13.0	11-15
Oct 16 - 31	10	8-12	12.0	9-14

VR Mainstem (AES-58 to AES-49)

Date	2007 Mean (°C)	2007 Range (°C)
June 16 - 30	13.0	11-15
July 1 - 15	14.0	11-15
July 16 - 31	14.0	12-16
Aug 1 - 15	15.0	13-17
Aug 16 - 31	15.0	13-17
Sep 1 - 15	15.0	13-16
Sep 16 - 30	14.0	13-15
Oct 1 - 15	13.0	12-15

South Branch (AES-23 to AES-21)

Date	2006 Mean (°C)	2006 Range (°C)	2007 Mean (°C)	2007 Range (°C)
June 1 - 15	--	--	13.0	10-14
June 16 - 30	--	--	13.0	11-15
July 1 - 15	--	--	14.0	11-15
July 16 - 31	--	--	14.0	12-16
Aug 1 - 15	--	--	15.0	13-17
Aug 16 - 31	--	--	15.0	13-17
Sep 1 - 15	12	9-14	15.0	13-16
Sep 16 - 30	11	9-14	14.0	13-15
Oct 1 - 15	11	8-13	13.0	12-15

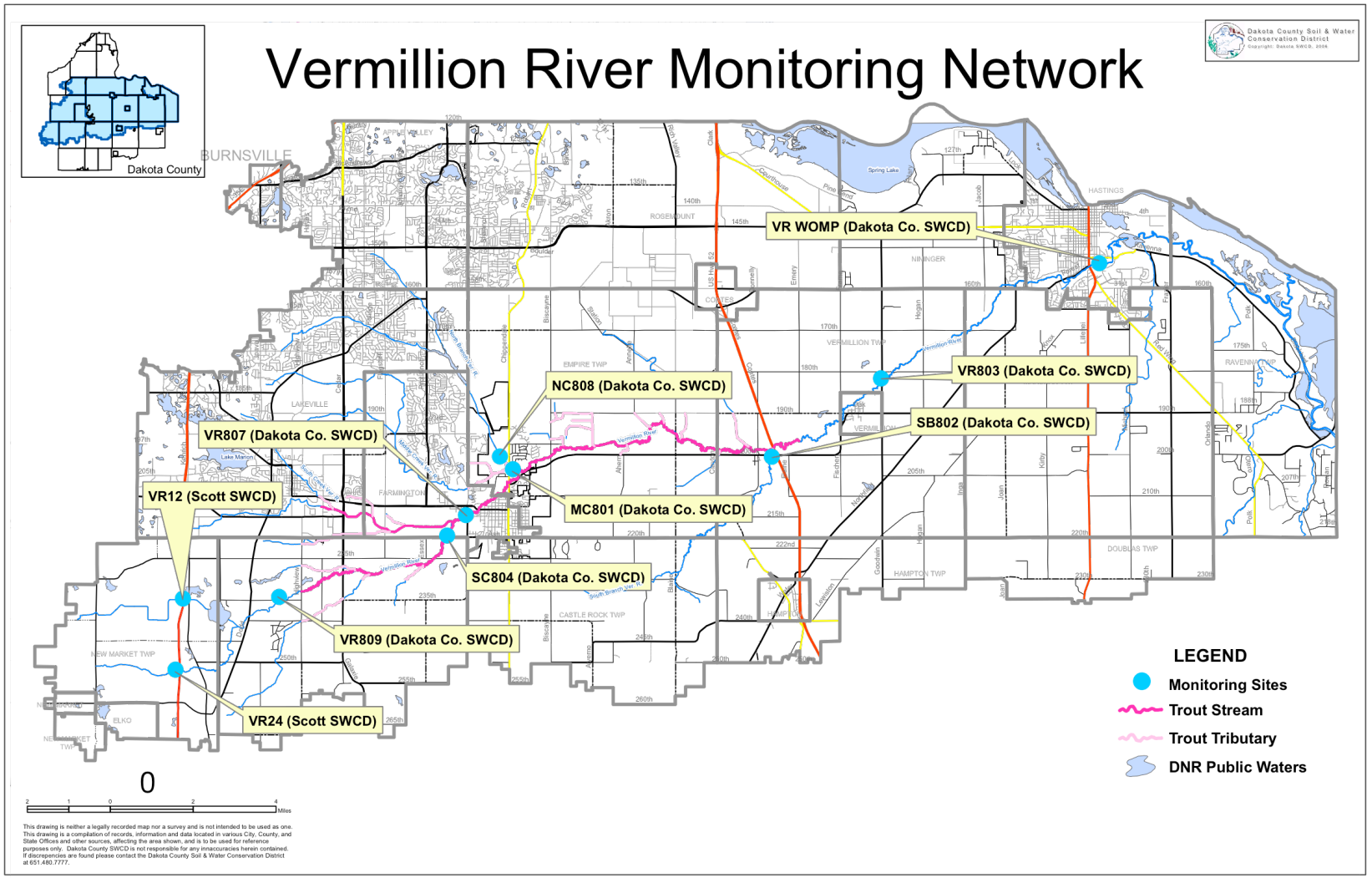

Figure A-1. Location of stream gaging stations in the Vermillion River watershed Courtesy of Dakota County Soil and Water Conservation District.

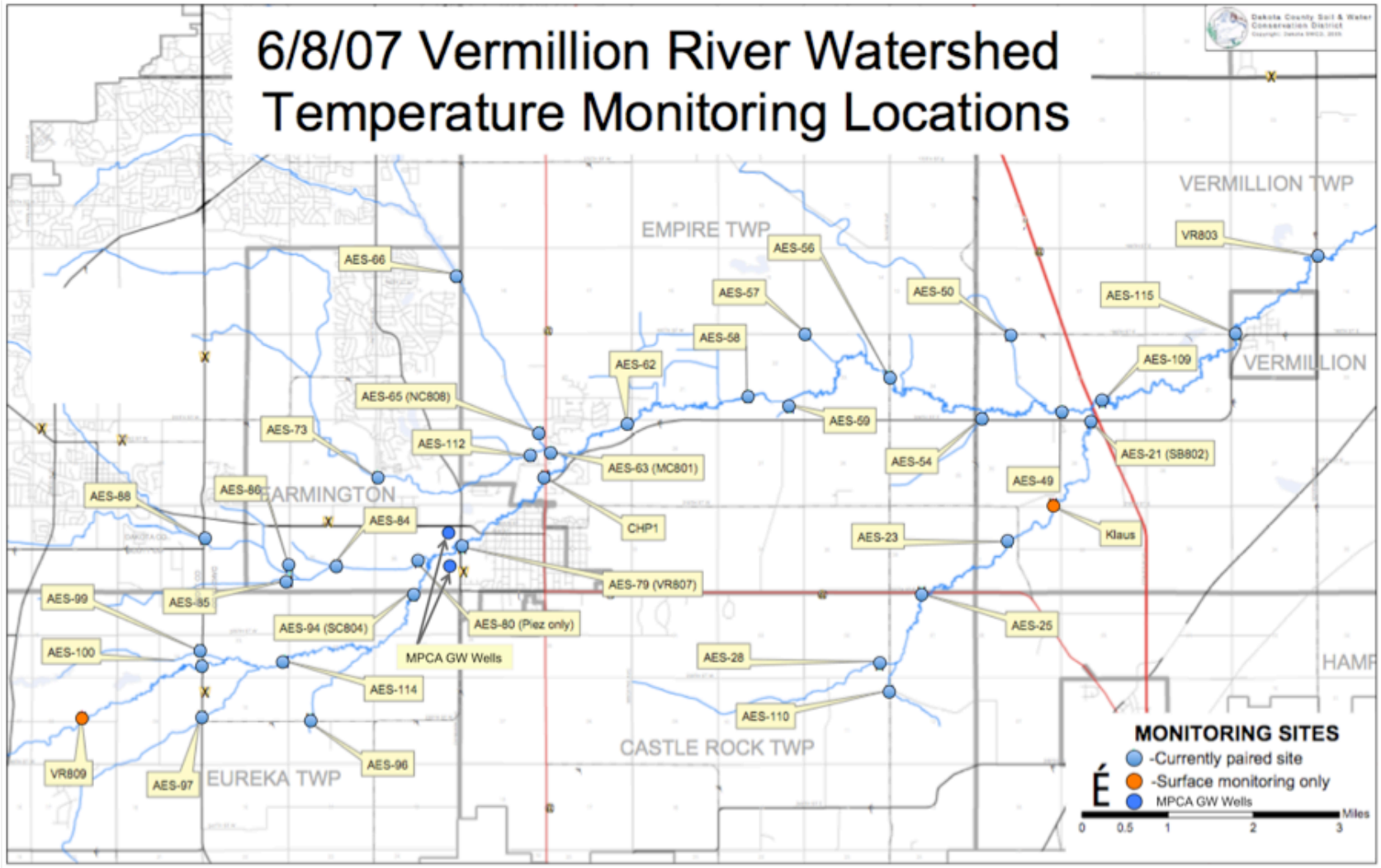

Figure A-2. Location of stream and groundwater temperature monitoring stations in the Vermillion River watershed as of June 8, 2007. Courtesy of Dakota County Soil and Water Conservation District.